

**Final Year Project  
Thesis**

**Title :  
Under-Cooling Vs Spacing relationship for  
the semi-regular brick Structure :  
Derivation and numerical simulations.**

*Submitted in partial fulfillment of  
the requirements for the award of the degree of*

**Bachelor of Science(Research)  
in  
Materials Science**

Submitted by

---

SR. No

Names of Students

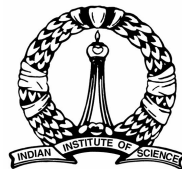
---

11-01-00-10-91-12-1-09921

Abhishek Kumar

---

Under the guidance of  
**Abhik N Chowdhury**



Department of Materials Engineering  
INDIAN INSTITUTE OF SCIENCE BANGALORE

# Department of Materials Engineering

INDIAN INSTITUTE OF SCIENCE BANGALORE

## *Certificate*

This is to certify that this is a bonafide record of the project presented by the student whose name is given below during term January and Year 2016 in partial fulfilment of the requirements of the degree of Bachelor of Science(Research) in Materials Science .

Roll No	Names of Students
11-01-00-10-91-12-1-09921	Abhishek Kumar

Abhik N Chowdhury  
(Project Guide)

Satyam Suwas  
(UG Coordinator, Materials)

Date:

# Acknowledgments

I would like to express my sincere gratitude to my project supervisor, Prof. Abhik Choudhury. Without his guidance and encouragement, this work could not have been done.

I wish to thank to all the members of Modelling group for their constant support during both good and difficult times.

I would like to thank all my course advisers and I have learned a lot from them.

I wish to thank my friends for their constant support . I also thank to all my 2012 batch mates.

Finally, I thank to my parents, for their constant support, love and encouragement throughout my study

## **Abstract**

A general theory for the growth of semi-regular, brick type structure is presented. These modes of growth depends on the interplay between the diffusion required for phase separation and the formation of interface boundaries. The present analysis of these factors provides a justification for earlier approximate theories. In order to consider a phase selection in a ternary eutectic system, analytical expression are derived for the three-phase planar growth have been derived, assuming the semi-regular type geometry. Lamellar three-phase patterns that form during the directional solidification of ternary eutectic alloys have many different geometric arrangement of three phase are possible in ternary eutectic. Here first derivation of Undercooling vs spacing relationship for the case of the semi-regular brick micro-structure that is seen during the three-phase growth, where the case of stable lamellar coupled growth of a symmetric model ternary alloy, using Jackson-Hunt type calculation for semi-regular configuration and derive expression of the interface-front undercooling as function of velocity and spacing. Next results of phase-field simulation and parametric study to test the analytical predictions are presented.

# Contents

<b>Acknowledgements</b>	<b>2</b>
<b>1 Problem Definition</b>	<b>1</b>
1.1 Derivation . . . . .	1
1.2 Comparison with Phase field simulation . . . . .	1
<b>2 Introduction</b>	<b>2</b>
2.1 Background . . . . .	2
2.1.1 Growth of lamellar eutectics . . . . .	2
2.1.2 Literature Survey . . . . .	3
2.2 Motivation . . . . .	3
<b>3 Derivation of Analytical solution</b>	<b>5</b>
3.1 Introduction . . . . .	5
3.1.1 Basic assumption and commom procedure . . . . .	5
3.1.2 Mass balance at the Interface and the temperature dif- ference owing to the solute . . . . .	6
3.2 Growth with Semi-regular,Brick type structure:Derivation . .	6
3.2.1 Formulation of the diffusion field problem and their solution . . . . .	6
3.2.2 Solving for $q_{nm}$ from the governing equation . . . . .	7
3.2.3 Calculation of the Fourier amplitude: $X_{nm}$ . . . . .	7
3.2.4 Calculation of $X_{nm}$ for different Fourier Modes . . . . .	11
3.2.5 Composition re-written using the symmetry property of the Periodic function . . . . .	12
3.3 Calculation of average composition of the component across interface for the calculation of undercooling . . . . .	15
3.3.1 Calculation of average composition of X=A,B,C in each phase . . . . .	16
3.4 Calculation of Average Curvature of interface of $\alpha$ $\beta$ and $\gamma$ -Phase	19
3.5 Expression for $\Delta T$ as a function of velocity and $\lambda$ . . . . .	21

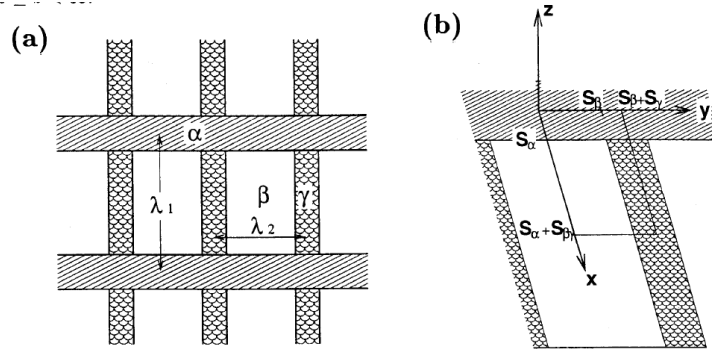
<b>4</b>	<b>Phase field simulation and parametric analysis</b>	<b>24</b>
4.1	Algorithm for undercooling and lambda Calculations . . . . .	24
4.2	Phase field simulation of evolution of semi-brick Structure . .	25
4.3	Comparison between: analytical and phase field results . . . .	26
4.4	Result for Symmetric phase diagram . . . . .	27
4.5	Result For Non-Symmetric phase diagram . . . . .	28
4.6	Parametric study : Undercooling vs $\lambda$ variation under the fol- lowing parametric changes . . . . .	29
4.6.1	Influence of contact angle's(which get fixed by suface energy) . . . . .	29
4.6.2	Influence of slopes(liquidus) . . . . .	32
4.6.3	Influence of velocity . . . . .	35
4.6.4	Effect of Volume fractions . . . . .	36
<b>5</b>	<b>Future Work</b>	<b>37</b>
<b>6</b>	<b>Conclusion</b>	<b>38</b>
<b>7</b>	<b>Appendix</b>	<b>39</b>
7.1	Appendix A . . . . .	39
7.2	Appendix B . . . . .	42
	<b>References</b>	<b>43</b>

# Chapter 1

## Problem Definition

### 1.1 Derivation

To Derive the expression for the undercooling vs Spacing relational ship for case of the semi-brick type morhpology which that is seen during the three-



phase growth.

Schematic Diagram of the three-Phase eutectic with semi-regular,brick-type structure.(taken from Ref.2)

(a) Its arrangement shown from the liquid ,

(b) Coordinate system.

Because of the symmetry in the given problem the aplha beta and gamma phase cab be interchanged. And the lenght of Domain can be taken full wavelenght instead of half wave length.

### 1.2 Comparison with Phase field simulation

# Chapter 2

## Introduction

Ternary eutectic Undercooling derivation: Semi Regular Brick Morphology Derivation for Undercooling vs spacing relationship for the semi-regular brick Structure that is seen during the three phase growth. To consider a phase selection in a ternary system eutectic system, analytical expressions for the three-phase planar eutectic growth, assuming the geometry as the semi-regular types, have been derived. The relations that the undercooling is proportional to the square root of the growth rate of the interface and that the structure size is inversely proportional to the square root of the growth. In the report the detailed procedure to derive the growth equation is described.

### 2.1 Background

#### 2.1.1 Growth of lamellar eutectics

The growth of lamellar eutectics has been the subject of several theoretical and many experimental studies. The foundations for theoretical work were laid by Zener and Brandt in their estimated the effect of the pearlite. Zener estimated the effect of diffusion, and took into account the surface energy of the lamellar structure. He found that the lamellar structure could grow in a range of growth rates at a given undercooling provided the lamellar spacing was appropriate for the growth. Zener removed this ambiguity by postulating that the growth rate was maximum possible at the given undercooling. Brandt was able to obtain an approximated solution to the diffusion equation, but since he did not take into account the surface energy. Hillert extended the work of Zener. He found a solution to the diffusion equation assuming the interface to be plane.

The diffusion equation predicts the existence of a diffusion boundary layer



at the eutectic interface unless the eutectic has half of the volume fraction of each phase and is growing into the eutectic composition. This boundary layer is such so to make the composition in the liquid at the interface approximately equal to the eutectic composition. This boundary layer permits changes in composition during the zone refining of eutectics. The boundary layer permits a eutectic structure to grow over a range of composition. Good agreement has been obtained between theory and experiments for the relationship between the lamellar spacing, growth rate, and interface undercooling.

### 2.1.2 Literature Survey

Following the Jackson and Hunt, Himemiya and Umeda assumed the local equilibrium at the solid-liquid interface. Therefore the undercooling at the eutectic front is assumed to be due to the composition difference  $\Delta T = \Delta T_c + \Delta T_\sigma$ , that is the total undercooling is given by the undercooling due to deviation from the initial (eutectic) composition plus the undercooling due to the Gibbs-Thomson effect (Curvature undercooling). The Kinetic undercooling as a driving force of atom attachment is neglected. In solving the diffusion equation, the interface of two solutes is neglected, that is, simple superposition of diffusion of the two solutes is assumed. The solid phase is assumed to grow at a constant velocity. Therefore the problem turns out to be a steady state. Himemiya and Umeda confirmed that the undercooling at the solid liquid interface is proportional to the square root of the growth rate, and the two spacing of the eutectic structure are inversely proportional to the square root of the growth rate.

## 2.2 Motivation

Three-phase, ternary eutectic growth has been a topic of high interest for both experimentalists as well as theoreticians owing to the rich variety of patterns or microstructures possible. Rigorous study of these microstructures can provide an improved understanding of the principle mechanisms of general importance for the development of multicomponent alloys needed in advanced technology applications. Experimental investigations of ternary alloys have been carried out for both metallic and inorganic alloys for thin-film solidification conditions. Bulk solidification of three-phase growth has also been studied extensively. However, theoretical investigations of three-phase growth have been few. Himemiya and Umeda have worked out analytical ex-

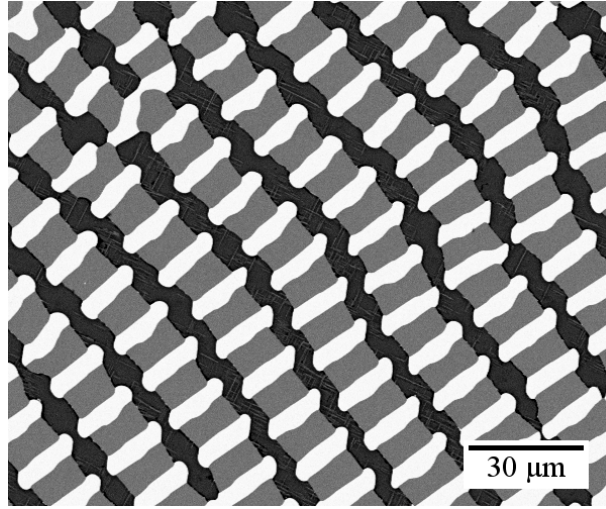


Figure 2.1: semi-brick morphology in Ag-Al-Cu a typical microstructure in a DS alloy

pressions for undercooling as a function of spacings for different three-phase configurations. One of the widely studied alloys in this regard is the Ag-Al-Cu alloy which classically shows patterns of the type as shown in Fig. However, there are other systems such as the Nb-Al-Ni ternary eutectic system [19] that exhibit quite different patterns compared to those seen in the Ag-Al-Cu alloy. These observations raise interesting questions regarding the correlation of microstructure features to material and/or processing parameters and during which the pattern at a given composition of the liquid is allowed to get reasonably close to the steady-state condition.

# Chapter 3

## Derivation of Analytical solution

### 3.1 Introduction

In ternary eutectic system, there exists three-phase macroscopically planar eutectic growth mode. To consider a phase selection in a ternary eutectic system, we have to calculate the temperature of the solidification front as a function of solidification conditions through the properties of the materials.

#### 3.1.1 Basic assumption and common procedure

Following the Jackson and Hunt analysis, the local equilibrium at the solid-liquid interface is assumed. Therefore, the Undercooling at the eutectic front is assumed to be  $\Delta T = \Delta T_c + \Delta T_\sigma$ , that is the total undercooling equals the undercooling due to the deviation from the solute content from the initial composition plus the undercooling due to the Gibbs-Thomson effect. For typical (slow) growth velocities that is attainable in directional solidification experiments the term due to the kinetic undercooling as a driving force of atom is neglected. In solving the diffusion problem, the cross-effect of two solutes is neglected, that is simple superposition is assumed to hold true. The solid phases are assumed to grow at a constant velocity. Therefore, the problem turns out to be steady-state. A simple ternary eutectic system is considered in this work, but the results of the derivation and simulation can also be extended into the region of three-phase eutectic in a ternary system.

As a common procedure for these cases, a five-step procedure is employed. The steps are: (1) to the diffusion field problem assuming that the solid-liquid interface is planar, (2) to estimate the mean curvature of the interface of each

phase,(3) to estimate the mean undercooling ahead of each interface,(4) to assume that undercooling of each phase is equal (i.e condition for the Isothermal solidification),assuming again that the eutectic front is macroscopically flat, and (5) to adopt the extreme condition(to assume the undercooling is minimum against the eutectic structure size).In metallic systems,the solute diffusion length is much less than the thermal diffusion length, and the growth of solid is governed by the solute diffusion. The diffusion of solutes can be approximately estimated by assuming the planar solid-liquid interface instead of the real solid-liquid interface.

### 3.1.2 Mass balance at the Interface and the temperature difference owing to the solute

The alloy having the initial composition  $(C_B^L, C_C^L)$  is assumed to solidify to form  $\alpha$ -phase( $C_{oB}^\alpha, C_{oC}^\beta$ ),  $\beta$ -phase, and  $\gamma$ -phase ( $C_{oB}^\gamma, C_{oC}^\gamma$ ). The volume fraction of the  $\alpha$ -phase is denoted by  $f_\alpha$ , that of the  $\beta$ -phase by  $f_\beta$  and that of  $\gamma$ -phase by  $f_\gamma$ . If the content of the three solid phases are assumed approximately to be these with the ternary eutectic triangle, then  $f_\alpha, f_\beta$  and  $f_\gamma$  could be determined.

## 3.2 Growth with Semi-regular,Brick type structure:Derivation

In this case of geometrical arrangement, a semi-regular,brick type structure is considered. In the case The  $\gamma$ -phase have thin film shape and between the  $\alpha$  and  $\beta$ -phase make up lamellar structure. The structure has two dimensional regularity so that we must consider the x-direction and y-direction.

### 3.2.1 Formulation of the diffusion field problem and their solution

The diffusion field problem of the solute X (=A,B,C) formulated as below the governing equation in the liquid which is written in a moving frame with a velocity  $V$  i.e,

$$\nabla^2 c_X + \frac{V}{D} \frac{\partial c_X}{\partial z} = 0. \quad (3.1)$$

where the  $D$  is the Diffusivity of the respective solute content. Note that the Laplacian operator is 3-Dimensional.

For the three-phase semi regular brick morphology we assume the composition profile described by the form,

$$c_X = C_E^X + \sum_{n=-\infty}^{\infty} \sum_{m=-\infty}^{\infty} X_{nm} e^{ik_n x} e^{ik_m y} e^{-q_{nm} z}, \quad (3.2)$$

where  $X$  denotes any of three elements  $A, B, C$  in the ternary alloy.  $X_{nm}$  are the amplitude of the respective modes denoted by  $n, m$ . The wavenumbers, corresponding to them by  $k_n = \frac{2n\pi}{\lambda_{\alpha\beta}}$  and  $k_m = \frac{2m\pi}{\lambda_{\alpha\beta+\gamma}}$  correspond to the repeat distance along the two lateral directions defining the semi-regular brick structure.  $-q_{nm}$  is the growth rate corresponding to the mode characterized by the  $nm$ .

The solution must satisfy the governing equation in the liquid.

### 3.2.2 Solving for $q_{nm}$ from the governing equation

substituting Eqn.3.2 into Eqn. 3.1

$$\begin{aligned} & \sum_{n=-\infty}^{\infty} \sum_{m=-\infty}^{\infty} [X_{nm} * (ik_n)^2 * e^{ik_n x} e^{ik_m y} e^{-q_{nm} z} + X_{nm} * (ik_m)^2 e^{ik_n x} e^{ik_m y} e^{-q_{nm} z}] \\ & + [(q_{nm})^2 X_{nm} * (ik_n)^2 * e^{ik_n x} e^{ik_m y} e^{-q_{nm} z} - \frac{V}{D} q_{nm} X_{nm} * (ik_n)^2 * e^{ik_n x} e^{ik_m y} e^{-q_{nm} z}] = 0 \end{aligned} \quad (3.3)$$

so the characteristic equation that we get

$$-k_n^2 - k_m^2 + q_{nm}^2 - \frac{V}{D} q_{nm} = 0 \quad (3.4)$$

solving the quadratic equation and taking only the positive root as we have assumed that the  $q_{nm}$  is positive for the decaying far field solution. So positive composition profile in far-field matches with imposed boundary condition.

$$q_{nm} = \frac{V}{2D} + \sqrt{\frac{V^2}{4D^2} + (k_n^2 + k_m^2)}. \quad (3.5)$$

### 3.2.3 Calculation of the Fourier amplitude: $X_{nm}$

Now let us define the Domain of our solution: Form the volume fraction we can get length of the  $\alpha, \beta$  and  $\gamma$ -phase.

For the  $\alpha$ -phase,  $x \in [0, \eta_\alpha \lambda_{\alpha\beta}]$   $y \in [0, \eta_{\alpha\beta} \lambda_{\alpha\beta}]$

For the  $\beta$ -phase,  $x \in [\eta_\alpha \lambda_{\alpha\beta}, \lambda_{\alpha\beta}]$   $y \in [0, \eta_{\alpha\beta} \lambda_{\alpha\beta}]$

For the gamma phase,  $x \in [0, \lambda_{\alpha\beta}]$   $y \in [\eta_{\alpha\beta} \lambda_{\alpha\beta}, \lambda_{\alpha\beta+\gamma}]$

from the calculated volume fraction the relational ship between  $\eta_\gamma$   $\eta_{\alpha\beta}$   $\eta_\alpha$  and  $\eta_\beta$  can be calculated.

$$\eta_\gamma = \mathbf{f}_\gamma, \quad (3.6)$$

$$\eta_{\alpha\beta} = (1.0 - \eta_\gamma) \quad (3.7)$$

$$\eta_\alpha = (\mathbf{f}_\alpha / (1.0 - \mathbf{f}_\gamma)) \quad (3.8)$$

$$\eta_\beta = (\mathbf{f}_\beta / (1.0 - \mathbf{f}_\gamma)) \quad (3.9)$$

The diffusion equation which is formulated for the solute X=(A,B,C) should the Boundary Conditions which is mentioned below:

$$C_X = C_X^L = C_X^E + C_X^\infty \quad \text{as } z \rightarrow \infty \quad (3.10)$$

$$\frac{\partial C_X}{\partial x} = 0 \quad \text{at } x = 0 \quad (3.11)$$

$$\frac{\partial C_X}{\partial x} = 0 \quad \text{at } x = \lambda_{\alpha\beta} \quad (3.12)$$

$$\frac{\partial C_X}{\partial y} = 0 \quad \text{at } y = 0 \quad (3.13)$$

$$\frac{\partial C_X}{\partial y} = 0 \quad \text{at } y = \lambda_{\alpha\beta+\gamma} \quad (3.14)$$

In order to derive the amplitude of the respective mode we can use the stefan's Condition: which also the conservation condition of the solute:-

$$\frac{\partial C_X}{\partial z} \Big|_{z=0} = \frac{V \Delta C_X^\alpha}{D_X} \quad \text{at } 0 < x < \eta_\alpha \lambda_{\alpha\beta} \quad 0 < y < \eta_{\alpha\beta} \lambda_{\alpha\beta+\gamma} \quad (3.15)$$

$$\frac{\partial C_X}{\partial z} \Big|_{z=0} = \frac{V \Delta C_X^\beta}{D_X} \quad \text{at } \eta_\beta \lambda_{\alpha\beta} < x < \lambda_{\alpha\beta} \quad 0 < y < \eta_{\alpha\beta} \lambda_{\alpha\beta+\gamma} \quad (3.16)$$

$$\frac{\partial C_X}{\partial z} \Big|_{z=0} = \frac{V \Delta C_X^\gamma}{D_X} \quad \text{at } 0 < x < \lambda_{\alpha\beta} \quad \eta_{\alpha\beta} \lambda_{\alpha\beta+\gamma} < y < \lambda_{\alpha\beta+\gamma} \quad (3.17)$$

$$\text{where } \Delta C_X^i = C_X^i - C_X^E \quad \text{here } E \text{ stands for eutectic} \quad (3.18)$$

Now the above mentioned equations can be written in compact notation for simpler calculations:

$$\partial_z c_X|_{z=0} = -\frac{V}{D} (c_X^l - c_X^\nu) = \frac{V}{D} (\Delta c_X^{\nu l}) \quad (3.19)$$

where  $l$  refers to the liquid and  $\nu$  refers to any of the solid phases that are in contact with the liquid. For all  $n \neq 0$  and  $m \neq 0$ , the amplitudes  $X_{nm}$  can be derived using the Stefan condition in the preceding relation and performing an inverse Fourier transform, Eqn. 3.2 into Eqn. 3.19

$$\frac{\partial}{\partial z} (C_E^X + \sum_{n=-\infty}^{\infty} \sum_{m=-\infty}^{\infty} X_{nm} e^{ik_n x} e^{ik_m y} e^{-q_{nm} z}) = \frac{V \Delta C_X^{\nu l}}{D} \quad (3.20)$$

$$0 + \sum_{n=-\infty}^{\infty} \sum_{m=-\infty}^{\infty} -q_{nm} X_{nm} e^{ik_n x} e^{ik_m y} e^{-q_{nm} z} = \frac{V \Delta C_X^{\nu l}}{D} \quad (3.21)$$

Now performing Inverse-Fourier Transfer: as RHS is known for the given periodicity in alpha we can make use Inverse-Fourier transfer to get  $X_{nm}$ , to do so multiply Equation(21) by a factor  $e^{-ik_n x} e^{-ik_m y}$  and performing integration over the repeat length.

$$\int_0^{\lambda_{\alpha\beta}} \int_0^{\lambda_{\alpha\beta}+\gamma} q_{nm} X_{nm} e^{ik_n x} e^{ik_m y} e^{-ik_n x} e^{-ik_m y} dx dy = \frac{V}{D} \int_0^{\lambda_{\alpha\beta}} \int_0^{\lambda_{\alpha\beta}+\gamma} \Delta c_X^{\nu l} e^{-i(k_n x + k_m y)} dx dy \quad (3.22)$$

$$q_{nm} X_{nm} \lambda_{\alpha\beta} \lambda_{\alpha\beta} + \gamma = \frac{V}{D} \int_0^{\lambda_{\alpha\beta}} \int_0^{\lambda_{\alpha\beta}+\gamma} \Delta c_X^{\nu l} e^{-i(k_n x + k_m y)} dx dy. \quad (3.23)$$

To solve the RHS we make use the periodic condition of repeated domain of each phase. Simplifying the Eqn. 3.23 by taking integration limits over different phase step by step.

For  $\alpha$ -Phase recall that the domain of integration  $x \in [0, \eta_{\alpha} \lambda_{\alpha\beta}]$   $y \in [0, \eta_{\alpha\beta} \lambda_{\alpha\beta}]$

$$\int_0^{\eta_{\alpha} \lambda_{\alpha\beta}} \int_0^{\eta_{\alpha\beta} \lambda_{\alpha\beta} + \gamma} \Delta c_X^{\alpha} e^{-i(k_n x + k_m y)} dx dy = \frac{V \Delta c_X^{\alpha}}{D} \frac{(e^{-ik_n \eta_{\alpha} \lambda_{\alpha\beta}} - 1)(e^{-ik_m \eta_{\alpha\beta} \lambda_{\alpha\beta} + \gamma} - 1)}{i^2 k_n k_m}$$

substituting for  $k_n$  and  $k_m = \frac{-V \Delta c_X^{\beta}}{D} \frac{(e^{-i2n\pi\eta_{\alpha}} - 1)(e^{-i2m\pi\eta_{\alpha\beta}} - 1)}{k_n k_m}$

For  $\beta$ -phase the integration domain  $x \in [\eta_\alpha \lambda_{\alpha\beta}, \lambda_{\alpha\beta}]$   $y \in [0, \eta_{\alpha\beta} \lambda_{\alpha\beta}]$

$$\int_{\eta_\alpha \lambda_{\alpha\beta}}^{\lambda_{\alpha\beta}} \int_0^{\eta_{\alpha\beta} \lambda_{\alpha\beta} + \gamma} \Delta c_X^\beta e^{(-i(k_n x + k_m y))} dx dy = \frac{V \Delta c_X^\alpha (e^{-ik_n \lambda_{\alpha\beta}} - e^{-ik_n \eta_\alpha \lambda_{\alpha\beta}})(e^{-ik_m \eta_\beta \lambda_{\alpha\beta} + \gamma} - 1)]}{D i^2 k_n k_m}$$

*substituting for  $k_n$  and  $k_m = \frac{-V \Delta c_X^\beta (1 - e^{-i2n\pi\eta_\alpha})(e^{-i2m\pi\eta_{\alpha\beta}} - 1)]}{D k_n k_m}$*

And for the  $\gamma$ -phase the Domain of integration  $x \in [0, \lambda_{\alpha\beta}]$   $y \in [\eta_{\alpha\beta} \lambda_{\alpha\beta}, \lambda_{\alpha\beta} + \gamma]$  it is worth to note that the contribution from the surface integral is zero for  $\gamma$  phase.

So after the simplification of RHS of equation 3.23 we get following equation,

$$q_{nm} X_{nm} \lambda_{\alpha\beta} \lambda_{\alpha\beta} + \gamma = \frac{V}{D} \left[ -\frac{\Delta c_X^\alpha}{k_n k_m} (e^{-i2\pi n \eta_\alpha} - 1) (e^{-i2\pi m \eta_{\alpha\beta}} - 1) \right] + \frac{V}{D} \left[ -\frac{\Delta c_X^\beta}{k_n k_m} (1 - e^{-i2\pi n \eta_\alpha}) (e^{-i2\pi m \eta_{\alpha\beta}} - 1) \right], \quad (3.24)$$

The above can be simplified into the following expressions,

$$X_{nm} = \frac{4V [\Delta c_X^\alpha - \Delta c_X^\beta]}{D k_n k_m q_{nm} \lambda_{\alpha\beta} \lambda_{\alpha\beta} + \gamma} \sin(\pi n \eta_\alpha) \sin(\pi m \eta_{\alpha\beta}) e^{-i\pi(n\eta_\alpha + m\eta_{\alpha\beta})}. \quad (3.25)$$



### 3.2.4 Calculation of $X_{nm}$ for different Fourier Modes

**Case 1:**  $n \neq 0$   $m \neq 0$

$$X_{nm} = \frac{4V \left[ \Delta c_X^\alpha - \Delta c_X^\beta \right]}{Dk_n k_m q_{nm} \lambda_{\alpha\beta} \lambda_{\alpha\beta+\gamma}} \sin(\pi n \eta_\alpha) \sin(\pi m \eta_{\alpha\beta}) e^{-i\pi(n\eta_\alpha + m\eta_{\alpha\beta})}. \quad (3.26)$$

**Case 2:**  $n = 0$   $m \neq 0$

For modes with  $n = 0$  and  $m \neq 0$ , the amplitudes  $X_{0m}$  can be derived as.

$$q_{0m} X_{0m} \lambda_{\alpha\beta} \lambda_{\alpha\beta+\gamma} = \frac{V}{D} \int_0^{\lambda_{\alpha\beta}} \int_0^{\lambda_{\alpha\beta+\gamma}} \Delta c_X e^{-ik_m y} dx dy, \quad (3.27)$$

where  $X_{0m}$  can be derived as, by splitting the integration to three different for the  $\alpha$   $\beta$  and  $\gamma$

**The integration over the three domain**

for  $\alpha$ -phase

$$\frac{V}{D} \int_0^{\eta_\alpha \lambda_{\alpha\beta}} \int_0^{\eta_{\alpha\beta} \lambda_{\alpha\beta+\gamma}} \Delta c_x^\alpha e^{-ik_n x} dx$$

for  $\beta$ -phase

$$\frac{V}{D} \int_{\eta_\alpha}^{\lambda_{\alpha\beta}} \int_0^{\eta_{\alpha\beta} \lambda_{\alpha\beta+\gamma}} \Delta c_x^\beta e^{-ik_n x} dx$$

for  $\gamma$ -phase

$$\frac{V}{D} \int_0^{\lambda_{\alpha\beta}} \int_{\eta_{\alpha\beta} \lambda_{\alpha\beta+\gamma}}^{\lambda_{\alpha\beta+\gamma}} \Delta c_x^\gamma e^{-ik_n x} dx$$

hence we get following result

$$X_{0m} = \frac{2V \left( \Delta c_X^\alpha \eta_\alpha \lambda_{\alpha\beta} + \Delta c_X^\beta \eta_\beta \lambda_{\alpha\beta} - \Delta c_X^\gamma \lambda_{\alpha\beta} \right)}{Dk_m q_{0m} \lambda_{\alpha\beta} \lambda_{\alpha\beta+\gamma}} \sin(m\pi \eta_{\alpha\beta}) e^{-im\pi \eta_{\alpha\beta}}. \quad (3.28)$$

**Case 3:**  $m = 0$   $n \neq 0$

Similarly, modes with  $n \neq 0$  and  $m = 0$  have amplitudes that read,

$$X_{n0} = \frac{2V \eta_{\alpha\beta} \left[ \Delta c_X^\alpha - \Delta c_X^\beta \right]}{Dk_n \lambda_{\alpha\beta} q_{n0}} \sin(n\pi \eta_\alpha) e^{-i\pi n \eta_\alpha}. \quad (3.29)$$

### 3.2.5 Composition re-written using the symmetry property of the Periodic function

So we claim the solution can be written as follows

$$\begin{aligned}
c_X &= c_X^\infty + X_{00} + \\
&\sum_{n=1}^{\infty} \sum_{m=1}^{\infty} [(X_{nm} + X_{-nm}) + (X_{n-m} + X_{-n-m})] \cos(k_m y) \cos(k_n x) \\
&+ i [(X_{nm} + X_{-nm}) - (X_{n-m} + X_{-n-m})] \sin(k_m y) \cos(k_n x) \\
&+ i [(X_{nm} - X_{-nm}) + (X_{n-m} - X_{-n-m})] \cos(k_m y) \sin(k_n x) \\
&- [(X_{nm} - X_{-nm}) - (X_{n-m} - X_{-n-m})] \sin(k_m y) \sin(k_n x) + \\
&\sum_{n=1}^{\infty} (X_{n0} + X_{-n0}) \cos(k_n x) + i (X_{n0} - X_{-n0}) \sin(k_n x) + \\
&\sum_{m=1}^{\infty} (X_{0m} + X_{0-m}) \cos(k_m y) + i (X_{0m} - X_{0-m}) \sin(k_m y). \quad (3.30)
\end{aligned}$$

Justification of claim: summation can be done by taking the positive and negative term of  $n$  and  $m$  combined in a way such that the summation can be written in compact way to truncate the summation from 1 to  $\infty$ . The term  $X_{00}$  still unknown that will be fixed in the later part of derivation.

Further simplification

$$\begin{aligned}
X_{nm} &= \frac{4V [\Delta c_X^\alpha - \Delta c_X^\beta]}{Dk_n k_m q_{nm} \lambda_{\alpha\beta} \lambda_{\alpha\beta+\gamma}} \sin(\pi n \eta_\alpha) \sin(\pi m \eta_{\alpha\beta}) e^{-i\pi(n\eta_\alpha + m\eta_{\alpha\beta})}. \\
X_{-nm} &= \frac{4V [\Delta c_X^\alpha - \Delta c_X^\beta]}{Dk_n k_m q_{nm} \lambda_{\alpha\beta} \lambda_{\alpha\beta+\gamma}} \sin(\pi n \eta_\alpha) \sin(\pi m \eta_{\alpha\beta}) e^{-i\pi n \eta_\alpha} e^{m\eta_{\alpha\beta}}.
\end{aligned}$$

adding the terms

$$\begin{aligned}
X_{nm} + X_{-nm} &= \frac{4V (\Delta c_x^\alpha - \Delta c_x^\beta) \sin(n\pi\eta_\alpha) \sin(m\pi\eta_{\alpha\beta})}{Dk_n k_m \lambda_{\alpha\beta} \lambda_{\alpha\beta+\gamma}} [e^{in\pi\eta_\alpha} e^{-im\pi\eta_{\alpha\beta}} + e^{-in\pi\eta_\alpha} e^{-im\pi\eta_{\alpha\beta}}] \\
&= \frac{4V (\Delta c_x^\alpha - \Delta c_x^\beta) \sin(n\pi\eta_\alpha) \sin(m\pi\eta_{\alpha\beta})}{Dk_n k_m \lambda_{\alpha\beta} \lambda_{\alpha\beta+\gamma}} [e^{-im\pi\eta_{\alpha\beta}} (e^{in\pi\eta_\alpha} + e^{-in\pi\eta_\alpha})] \\
&= \frac{4V (\Delta c_x^\alpha - \Delta c_x^\beta) \sin(n\pi\eta_\alpha) \sin(m\pi\eta_{\alpha\beta})}{Dk_n k_m \lambda_{\alpha\beta} \lambda_{\alpha\beta+\gamma}} [e^{-im\pi\eta_{\alpha\beta}} (2\cos(n\pi\eta_\alpha))] \\
&= \frac{4V (\Delta c_x^\alpha - \Delta c_x^\beta) \sin(n\pi\eta_\alpha) \sin(m\pi\eta_{\alpha\beta}) (2\cos(n\pi\eta_{\alpha\beta}))}{Dk_n k_m \lambda_{\alpha\beta} \lambda_{\alpha\beta+\gamma}} [e^{-im\pi\eta_{\alpha\beta}}] \\
&= \frac{4V (\Delta c_x^\alpha - \Delta c_x^\beta) \sin(2n\pi\eta_\alpha) \sin(m\pi\eta_{\alpha\beta})}{Dk_n k_m \lambda_{\alpha\beta} \lambda_{\alpha\beta+\gamma}} [e^{-im\pi\eta_{\alpha\beta}}] \quad (3.31)
\end{aligned}$$

Similarly we can solve for the other term:

$$X_{n-m} = \frac{4V [\Delta c_X^\alpha - \Delta c_X^\beta]}{Dk_n k_m q_{nm} \lambda_{\alpha\beta} \lambda_{\alpha\beta+\gamma}} \sin(\pi n\eta_\alpha) \sin(\pi m\eta_{\alpha\beta}) e^{-i\pi(n\eta_\alpha - m\eta_{\alpha\beta})}.$$

$$X_{-n-m} = \frac{4V [\Delta c_X^\alpha - \Delta c_X^\beta]}{Dk_n k_m q_{nm} \lambda_{\alpha\beta} \lambda_{\alpha\beta+\gamma}} \sin(\pi n\eta_\alpha) \sin(\pi m\eta_{\alpha\beta}) e^{i\pi n\eta_\alpha} e^{m\eta_{\alpha\beta}}.$$

adding the two terms

$$X_{n-m} + X_{-n-m} = \frac{4V [\Delta c_X^\alpha - \Delta c_X^\beta]}{Dk_n k_m q_{nm} \lambda_{\alpha\beta} \lambda_{\alpha\beta+\gamma}} [\sin(2n\pi\eta_\alpha) e^{im\pi\eta_{\alpha\beta}}] \quad (3.32)$$

so eqn.(31) and eqn.(32) can be combined to give the following result

$$(X_{nm} + X_{-nm}) + (X_{n-m} + X_{-n-m}) = \frac{4V [\Delta c_X^\alpha - \Delta c_X^\beta]}{Dk_n k_m q_{nm} \lambda_{\alpha\beta} \lambda_{\alpha\beta+\gamma}} [\sin(2m\pi\eta_{\alpha\beta}) \sin(2\pi\eta_\alpha)] \quad (3.33)$$

similarly we can combine and add the other  $X_{nm}$  terms as follows

$$i(X_{nm} + X_{-nm}) - (X_{n-m} + X_{-n-m}) = \frac{4V \left[ \Delta c_X^\alpha - \Delta c_X^\beta \right]}{Dk_n k_m q_{nm} \lambda_{\alpha\beta} \lambda_{\alpha\beta+\gamma}} [2\sin(2n\pi\eta_\alpha) \sin(m\pi\eta_{\alpha\beta})^2] \quad (3.34)$$

$$i(X_{nm} - X_{-nm}) + (X_{n-m} - X_{-n-m}) = \frac{4V \left[ \Delta c_X^\alpha - \Delta c_X^\beta \right]}{Dk_n k_m q_{nm} \lambda_{\alpha\beta} \lambda_{\alpha\beta+\gamma}} [2\sin(2n\pi\eta_\alpha)^2 \sin(m\pi\eta_{\alpha\beta})] \quad (3.35)$$

$$-(X_{nm} - X_{-nm}) - (X_{n-m} - X_{-n-m}) = \frac{4V \left[ \Delta c_X^\alpha - \Delta c_X^\beta \right]}{Dk_n k_m q_{nm} \lambda_{\alpha\beta} \lambda_{\alpha\beta+\gamma}} [4\sin(2n\pi\eta_\alpha)^2 \sin(m\pi\eta_{\alpha\beta})^2] \quad (3.36)$$

$$(X_{n0} + X_{-n0}) = \frac{2V\eta \left[ \Delta c_X^\alpha - \Delta c_X^\beta \right]}{Dk_n q_{n0} \lambda_{\alpha\beta}} [\sin(2n\pi\eta_\alpha)] \quad (3.37)$$

$$i(X_{n0} - X_{-n0}) = \frac{2V\eta \left[ \Delta c_X^\alpha - \Delta c_X^\beta \right]}{Dk_n q_{n0} \lambda_{\alpha\beta}} [2\sin(n\pi\eta_\alpha)^2] \quad (3.38)$$

$$(X_{0m} + X_{0-m}) = \frac{2V\eta \left[ \Delta c_X^\alpha \eta_\alpha + \Delta c_X^\beta \beta - \Delta c_X^\gamma \right]}{Dk_m q_{0m} \lambda_{\alpha\beta}} [\sin(2m\pi\eta_{\alpha\beta})] \quad (3.39)$$

$$i(X_{0m} - X_{0-m}) = \frac{2V\eta \left[ \Delta c_X^\alpha \eta_\alpha + \Delta c_X^\beta \beta - \Delta c_X^\gamma \right]}{Dk_m q_{0m} \lambda_{\alpha\beta}} [2\sin(m\pi\eta_{\alpha\beta})] \quad (3.40)$$

Using the expression for the amplitudes that were developed earlier we can simply the preceding relation for the composition profiles as:

$$\begin{aligned}
c_X = c_X^\infty + X_{00} + & \\
\frac{4V \left[ \Delta c_X^\alpha - \Delta c_X^\beta \right]}{Dk_n k_m q_{nm} \lambda_{\alpha\beta} \lambda_{\alpha\beta+\gamma}} \sum_{n=1}^{\infty} \sum_{m=1}^{\infty} \left( \sin(2m\pi\eta_{\alpha\beta}) \sin(2n\pi\eta_\alpha) \cos(k_m y) \sin(k_n x) + \right. & \\
2 \sin(2n\pi\eta_\alpha) \sin^2(m\pi\eta_{\alpha\beta}) \sin(k_m y) \cos(k_n x) + & \\
2 \sin^2(n\pi\eta_\alpha) \sin(2m\pi\eta_{\alpha\beta}) \cos(k_m y) \sin(k_n x) + & \\
\left. 4 \sin^2(n\pi\eta_\alpha) \sin^2(m\pi\eta_{\alpha\beta}) \sin(k_m y) \sin(k_n y) \right) + & \\
\frac{2V \eta_{\alpha\beta} \left[ \Delta c_X^\alpha - \Delta c_X^\beta \right]}{Dk_n q_{n0} \lambda_{\alpha\beta}} \sum_{n=1}^{\infty} \left( \sin(2n\pi\eta_\alpha) \cos(k_n x) + 2 \sin^2(n\pi\eta_\alpha) \sin(k_n x) \right) + & \\
\frac{2V \left[ \Delta c_X^\alpha \eta_\alpha + \Delta c_X^\beta \eta_\beta - \Delta c^\gamma \right]}{Dk_m q_{0m} \lambda_{\alpha\beta+\gamma}} \sum_{m=1}^{\infty} \left( \sin(2m\pi\eta_{\alpha\beta}) \cos(k_m y) + 2 \sin^2(m\pi\eta_{\alpha\beta}) \sin(k_m y) \right). &
\end{aligned} \tag{3.41}$$

### 3.3 Calculation of average composition of the component across interface for the calculation of undercooling

From the preceding relation the composition profiles of each component can be derived. In order to compute the undercooling of a given solid-liquid interface, we require the average composition of that component across that interface. This average can be numerically be defined as,

$$\begin{aligned}
\langle c_X \rangle^\alpha &= \frac{\int_0^{\eta_\alpha \lambda_{\alpha\beta}} \int_0^{\eta_{\alpha\beta} \lambda_{\alpha\beta+\gamma}} c_X^\alpha dx dy}{\eta_\alpha \eta_{\alpha\beta} \lambda_{\alpha\beta} \lambda_{\alpha\beta+\gamma}} \\
\langle c_X \rangle^\beta &= \frac{\int_{\eta_\alpha \lambda_{\alpha\beta}}^{\lambda_{\alpha\beta}} \int_0^{\eta_{\alpha\beta} \lambda_{\alpha\beta+\gamma}} c_X^\beta dx dy}{\eta_\beta \eta_{\alpha\beta} \lambda_{\alpha\beta} \lambda_{\alpha\beta+\gamma}} \\
\langle c_X \rangle^\gamma &= \frac{\int_0^{\lambda_{\alpha\beta}} \int_{\eta_{\alpha\beta} \lambda_{\alpha\beta+\gamma}}^{\lambda_{\alpha\beta+\gamma}} c_X^\gamma dx dy}{\eta_\gamma \lambda_{\alpha\beta} \lambda_{\alpha\beta+\gamma}}.
\end{aligned} \tag{3.42}$$

### 3.3.1 Calculation of average composition of X=A,B,C in each phase

Case:1 Average composition in  $\alpha$ -phase

substituting the Composition term from eqn.41 into the  $\alpha$ -Phase average in eqn.42 it is worth to note that the constant terms would not contribute in average, so for simpler calculation we can take only the term containing the x and y variable.

$$\begin{aligned}
term1 &= \int_0^{\eta_\alpha \lambda_{\alpha\beta}} \int_0^{\eta_{\alpha\beta} \lambda_{\alpha\beta+\gamma}} \cos(k_m y) \cos(k_n x) dx dy \\
&= \left( \int_0^{\eta_\alpha \lambda_{\alpha\beta}} \cos(k_n x) dx \right) \left( \int_0^{\eta_{\alpha\beta} \lambda_{\alpha\beta+\gamma}} \cos(k_m y) dy \right) \\
&= \frac{\sin(2n\pi\eta_\alpha) \sin(2m\pi\eta_{\alpha\beta})}{k_n k_m} \\
term2 &= \int_0^{\eta_\alpha \lambda_{\alpha\beta}} \int_0^{\eta_{\alpha\beta} \lambda_{\alpha\beta+\gamma}} \sin(k_m y) \cos(k_n x) dx dy = 2 \sin(2n\pi\eta_\alpha) \sin(m\pi\eta_{\alpha\beta}) / (k_n k_m) \\
term3 &= \int_0^{\eta_\alpha \lambda_{\alpha\beta}} \int_0^{\eta_{\alpha\beta} \lambda_{\alpha\beta+\gamma}} \cos(k_m y) \sin(k_n x) dx dy = 2 \sin(n\pi\eta_\alpha)^2 \sin(2m\pi\eta_{\alpha\beta}) / (k_n k_m) \\
term4 &= \int_0^{\eta_\alpha \lambda_{\alpha\beta}} \int_0^{\eta_{\alpha\beta} \lambda_{\alpha\beta+\gamma}} \sin(k_m y) \sin(k_n x) dx dy = 4 \sin(n\pi\eta_\alpha)^2 \sin(m\pi\eta_{\alpha\beta}) / (k_n k_m) \\
term5 &= \int_0^{\eta_\alpha \lambda_{\alpha\beta}} \int_0^{\eta_{\alpha\beta} \lambda_{\alpha\beta+\gamma}} \cos(k_n x) dx dy = \sin(2n\pi\eta_\alpha) \eta_{\alpha\beta} \lambda_{\alpha\beta+\gamma} / (k_n) \\
term6 &= \int_0^{\eta_\alpha \lambda_{\alpha\beta}} \int_0^{\eta_{\alpha\beta} \lambda_{\alpha\beta+\gamma}} \sin(k_n x) dx dy = 2 \sin(n\pi\eta_\alpha)^2 \eta_{\alpha\beta} \lambda_{\alpha\beta+\gamma} / (k_n) \\
term7 &= \int_0^{\eta_\alpha \lambda_{\alpha\beta}} \int_0^{\eta_{\alpha\beta} \lambda_{\alpha\beta+\gamma}} \cos(k_m y) dy dx = \sin(2m\pi\eta_{\alpha\beta}) \eta_\alpha \lambda_{\alpha\beta} / (k_m) \\
term8 &= \int_0^{\eta_\alpha \lambda_{\alpha\beta}} \int_0^{\eta_{\alpha\beta} \lambda_{\alpha\beta+\gamma}} \sin(k_m y) dy dx = 2 \sin(m\pi\eta_{\alpha\beta})^2 \eta_\alpha \lambda_{\alpha\beta} / (k_m)
\end{aligned}$$

Similar treatment can be done for  $\eta$  and  $\gamma$  phase but we will use the symmetry of our problem and define a shorthand expression that will be helpful in carrying summation and integrals. So we define the following integrals

$$P(\eta_\alpha, \eta_{\alpha\beta}) = \sum_{n=1}^{\infty} \sum_{m=1}^{\infty} \frac{\sin^2(2m\pi\eta_{\alpha\beta}) \sin^2(2n\pi\eta_\alpha)}{k_n^2 k_m^2 \sqrt{k_n^2 + k_m^2}} \quad (3.43)$$

$$Q(\eta_\alpha, \eta_{\alpha\beta}) = \sum_{n=1}^{\infty} \sum_{m=1}^{\infty} \frac{\sin^2(2n\pi\eta_\alpha) \sin^4(m\pi\eta_{\alpha\beta})}{k_n^2 k_m^2 \sqrt{k_n^2 + k_m^2}} \quad (3.44)$$

$$R(\eta_{\alpha\beta}, \eta_\alpha) = \sum_{n=1}^{\infty} \sum_{m=1}^{\infty} \frac{\sin^4(n\pi\eta_\alpha) \sin^2(2m\pi\eta_{\alpha\beta})}{k_n^2 k_m^2 \sqrt{k_n^2 + k_m^2}} \quad (3.45)$$

$$X(\eta_{\alpha\beta}, \eta_\alpha) = \sum_{n=1}^{\infty} \sum_{m=1}^{\infty} \frac{\sin^4(n\pi\eta_\alpha) \sin^4(m\pi\eta_{\alpha\beta})}{k_n^2 k_m^2 \sqrt{k_n^2 + k_m^2}} \quad (3.46)$$

$$S(\eta_\alpha) = \sum_{n=1}^{\infty} \frac{\sin^2(2n\pi\eta_\alpha)}{k_n^3} \quad (3.47)$$

$$T(\eta_\alpha) = \sum_{n=1}^{\infty} \frac{\sin^4(n\pi\eta_\alpha)}{k_n^3} \quad (3.48)$$

$$U(\eta_{\alpha\beta}) = \sum_{m=1}^{\infty} \frac{\sin^2(2m\pi\eta_{\alpha\beta})}{k_m^3} \quad (3.49)$$

$$W(\eta_{\alpha\beta}) = \sum_{m=1}^{\infty} \frac{\sin^4(m\pi\eta_{\alpha\beta})}{k_m^3} \quad (3.50)$$

Finally we can write the average composition in  $\alpha$   $\beta$  and *gamma* phase as following:

$$\begin{aligned} \langle c_X \rangle^\alpha &= c_X^\infty + X_{00} + \\ &\quad \frac{4V \left[ \Delta c_X^\alpha - c_X^\beta \right]}{D \lambda_{\alpha\beta}^2 \lambda_{\alpha\beta+\gamma}^2 \eta_\alpha \eta_{\alpha\beta+\gamma}} [P(\eta_\alpha, \eta_{\alpha\beta}) + 4Q(\eta_\alpha, \eta_{\alpha\beta}) + 4R(\eta_\alpha, \eta_{\alpha\beta}) + 16X(\eta_\alpha, \eta_\alpha)] \\ &\quad + \frac{2V \eta_{\alpha\beta} \left[ \Delta c_X^\alpha - \Delta c_X^\beta \right]}{D \lambda_{\alpha\beta}^2 \eta_\alpha} [S(\eta_\alpha) + 4T(\eta_\alpha)] + \frac{2V \left( \Delta c_X^\alpha \eta_\alpha + \Delta c_X^\beta \eta_\beta - \Delta c_X^\gamma \right)}{D \eta_{\alpha\beta} \lambda_{\alpha\beta+\gamma}^2} [U(\eta_{\alpha\beta}) + 4W(\eta_{\alpha\beta})] \end{aligned} \quad (3.51)$$

$$\begin{aligned} \langle c_X \rangle^\beta &= c_X^\infty + X_{00} \\ &\quad - \frac{4V \left[ \Delta c_X^\alpha - c_X^\beta \right]}{D \lambda_{\alpha\beta}^2 \lambda_{\alpha\beta+\gamma}^2 \eta_\beta \eta_{\alpha\beta+\gamma}} [P(\eta_\alpha, \eta_{\alpha\beta}) + 4Q(\eta_\alpha, \eta_{\alpha\beta}) + 4R(\eta_\alpha, \eta_{\alpha\beta}) + 16X(\eta_\alpha, \eta_\alpha)] \\ &\quad - \frac{2V \eta_{\alpha\beta} \left[ \Delta c_X^\alpha - \Delta c_X^\beta \right]}{D \lambda_{\alpha\beta}^2 \eta_\beta} [S(\eta_\alpha) + 4T(\eta_\alpha)] + \frac{2V \left( \Delta c_X^\alpha \eta_\alpha + \Delta c_X^\beta \eta_\beta - \Delta c_X^\gamma \right)}{D \eta_{\alpha\beta} \lambda_{\alpha\beta+\gamma}^2} [U(\eta_{\alpha\beta}) + 4W(\eta_{\alpha\beta})] \end{aligned} \quad (3.52)$$

$$\langle c_X \rangle^\gamma = c_X^\infty + X_{00} - \frac{2V \left( \Delta c_X^\alpha \eta_\alpha + \Delta c_X^\beta \eta_\beta - \Delta c_X^\gamma \right)}{D \eta_\gamma \lambda_{\alpha\beta+\gamma}^2} [U(\eta_{\alpha\beta}) + 4W(\eta_{\alpha\beta})] \quad (3.53)$$



### 3.4 Calculation of Average Curvature of interface of $\alpha$ $\beta$ and $\gamma$ -Phase

If we define the mean Curvature of a surface as

$$\kappa = \frac{\kappa_1 + \kappa_2}{2} \quad (3.54)$$

the undercooling due to the Gibbs-Thomson effect will be

$$\Delta T_\sigma = 2\Gamma\kappa$$

where the  $\Gamma$  is the Gibbs-Thomson coefficient and  $\kappa_1$  and  $\kappa_2$  are the principle curvature. If we express the position of the interface as  $\zeta(x, y)$ , then  $\kappa_1$  or  $\kappa_2$  is:

$$\kappa_1 = \frac{-\frac{\partial^2 \zeta}{\partial x^2}}{[(\frac{\partial \zeta}{\partial x})^2 + 1]^{3/2}}$$

and

$$\kappa_2 = \frac{-\frac{\partial^2 \zeta}{\partial y^2}}{[(\frac{\partial \zeta}{\partial y})^2 + 1]^{3/2}}$$

A simpler calculation of curvature can be done by the geometric considerations of the  $\alpha$   $\beta$  and  $\gamma$  phase and the contact angles. So let us define the contact angle as follow

$\theta_{\alpha\beta}$  the contact angle between the  $\alpha - \beta$  interface

$\theta_{\alpha\gamma}$  the contact angle between the  $\alpha - \gamma$  interface

$\theta_{\beta\gamma}$  the contact angle between the  $\beta - \gamma$  interface

$\theta_{\beta\alpha}$  the contact angle between the  $\beta - \alpha$  interface

$\theta_{\gamma\alpha}$  the contact angle between the  $\gamma - \alpha$  interface

$\theta_{\gamma\beta}$  the contact angle between the  $\gamma - \beta$  interface

So have following relationship for the Curvature and the Surface energy term

$$\Gamma^\alpha \langle \kappa \rangle^\alpha = \Gamma^\alpha \left[ \frac{2 \sin(\theta_{\alpha\gamma})}{\eta_{\alpha\beta} \lambda_{\alpha\beta+\gamma}} + \frac{2 \sin(\theta_{\alpha\beta})}{\eta_\alpha \lambda_{\alpha\beta}} \right] \quad (3.55)$$

$$\Gamma^\beta \langle \kappa \rangle^\beta = \Gamma^\beta \left[ \frac{2 \sin(\theta_{\beta\gamma})}{\eta_{\alpha\beta} \lambda_{\alpha\beta+\gamma}} + \frac{2 \sin(\theta_{\beta\alpha})}{\eta_\beta \lambda_{\alpha\beta}} \right] \quad (3.56)$$

$$\Gamma^\gamma \langle \kappa \rangle^\gamma = \Gamma^\gamma \left[ \frac{2 \sin(\theta_{\gamma\alpha})}{\eta_\gamma \lambda_{\alpha\beta+\gamma}} + \frac{2 \sin(\theta_{\gamma\beta})}{\eta_\gamma \lambda_{\alpha\beta+\gamma}} \right] \quad (3.57)$$

$$(3.58)$$

here the  $\langle \kappa \rangle$  is evaluated by exact geometric relations where the contact angle at the triple point are applied by applying the Young's law at triple junction points. A short digression is in order to motivate the closure of our systems of equations. If we recall the fourier summation terms the term Containing  $X$  with  $n=0$  and  $m=0$  was not fixed, and explicit expression was not given, the coefficients  $A_0$  and  $B_0$  can be calculated by putting  $n=0$ . To carry out that calculations, the width of each lamella has to be given. If these widths are chosen consistent with the lever rule i.e the cumulative lamellar width of phase  $\nu$  corresponds to the nominal volume fraction of phase  $\nu$  for the sample concentration  $c_A^\infty, c_B^\infty, c_C^\infty$  which yields  $X_0 = c_X^E - c_X^\infty$   $X = A, B, C$ . However the result would be incorrect as the concentration of the solid are not equal to the equilibrium concentrations at the eutectic temperature because solidification takes place at a temperature below  $T_E$ , Therefore, the true volume fractions depend on the solidification conditions. Their determination would require a self-consistent calculation, which is exceedingly difficult. Therefore we will take same path as Jackson and Hunt in there original paper. We will assume that volume fraction of the three phase are fixed by the lever rule at the eutectic temperature, but we will treat the amplitudes of the two boundary layer term  $A_0$  and  $B_0$  as unknowns .

With these assumption, the equations developed above can now used in two ways. For isothermal solidification, the temperatures of all interface must be equals to the externally set temperature, and the three equation  $\Delta T_\nu = \Delta T$  for  $\nu = \alpha, \beta, \gamma$  can be used to determine the three unknowns  $A_0, B_0$  and the velocity  $\nu$  of the solid-liquid front. All of these quantities will be a function of lamellar spacing  $\lambda$ . In Directional solification, the growth velocity in steady state is fixed and equal to the speed with which the sample is pulled from a hot to a cold region. The third unknown is now the total front undercooling. Im the classic Jackson-Hunt theory for binary eutectic, the system of equations is closed by the hypothesis that the average undercooling of the two phase equal. This is only an approximation, which is quite accurate for the eutectics with comparable volume fractions of the two solids, but becomes increasingly inaccurate when the volume fraction are asymmetric . We will use the same approximation for the ternary case here to set  $\Delta T_\nu = \Delta T$ . This then leads to expression for  $\Delta T$  as a function of the growth speed and  $\lambda$ .

### 3.5 Expression for $\Delta T$ as a function of velocity and $\lambda$

From the general formulation of Gibbs-Thomson equations and using the above expressions for the average compositions and the curvature undercoolings the undercooling at each interface can be derived as,

$$\Delta T^\nu = -m_A^\nu (\langle c_A \rangle^\nu - c_A^E) - m_B^\nu (\langle c_B \rangle^\nu - c_B^E) + \Gamma^\nu \langle \kappa \rangle^\nu, \quad (3.59)$$

where  $\nu$  refers to any of the solid-phases from the set,  $\{\alpha, \beta, \gamma\}$ .

The only thing that remains is the values of the constants  $X_{00}$ . As in the classical JH analysis, we will leave these as unknowns, which can be fixed by the criterion that the undercooling at all the three interfaces are equal. So

$$\Delta T^\alpha = -m_A^\alpha (\langle c_A \rangle^\alpha - c_A^E) - m_B^\alpha (\langle c_B \rangle^\alpha - c_B^E) + \Gamma^\alpha \langle \kappa \rangle^\alpha, \quad (3.60)$$

$$\Delta T^\beta = -m_A^\beta (\langle c_A \rangle^\beta - c_A^E) - m_B^\beta (\langle c_B \rangle^\beta - c_B^E) + \Gamma^\beta \langle \kappa \rangle^\beta, \quad (3.61)$$

$$\Delta T^\gamma = -m_A^\gamma (\langle c_A \rangle^\gamma - c_A^E) - m_B^\gamma (\langle c_B \rangle^\gamma - c_B^E) + \Gamma^\gamma \langle \kappa \rangle^\gamma, \quad (3.62)$$

Under the assumption that  $\Delta T^\alpha = \Delta T^\beta = \Delta T^\gamma = \Delta T$  The expression for the

undercooling at the interface can be derived as,

$$\begin{aligned}
term1 = & \frac{\langle c_A \rangle^\beta - \langle c_B \rangle^\alpha}{\frac{m_B^\beta}{m_A^\beta} - \frac{m_B^\alpha}{m_A^\alpha}} - \frac{\langle c_A \rangle^\gamma - \langle c_B \rangle^\alpha}{\frac{m_B^\gamma}{m_A^\gamma} - \frac{m_B^\alpha}{m_A^\alpha}} + \\
& \frac{\left( \frac{m_B^\beta}{m_A^\beta} (\langle c_B \rangle^\beta - X_{00} - c_B^E) - \frac{m_B^\alpha}{m_A^\alpha} (\langle c_B \rangle^\alpha - X_{00} - c_B^E) \right)}{\frac{m_B^\beta}{m_A^\beta} - \frac{m_B^\alpha}{m_A^\alpha}} + \\
& - \frac{\left( \frac{m_B^\gamma}{m_A^\gamma} (\langle c_B \rangle^\gamma - X_{00} - c_B^E) - \frac{m_B^\alpha}{m_A^\alpha} (\langle c_B \rangle^\alpha - X_{00} - c_B^E) \right)}{\frac{m_B^\gamma}{m_A^\gamma} - \frac{m_B^\alpha}{m_A^\alpha}} + \\
& \frac{\frac{\Gamma^\alpha \kappa^\alpha}{m_A^\alpha} - \frac{\Gamma^\beta \kappa^\beta}{m_A^\beta}}{\frac{m_B^\beta}{m_A^\beta} - \frac{m_B^\alpha}{m_A^\alpha}} - \frac{\frac{\Gamma^\alpha \kappa^\alpha}{m_A^\alpha} - \frac{\Gamma^\gamma \kappa^\gamma}{m_A^\gamma}}{\frac{m_B^\gamma}{m_A^\gamma} - \frac{m_B^\alpha}{m_A^\alpha}} \\
term2 = & \left\{ \frac{\frac{1}{m_A^\alpha} - \frac{1}{m_A^\beta}}{\frac{m_B^\beta}{m_A^\beta} - \frac{m_B^\alpha}{m_A^\alpha}} - \frac{\frac{1}{m_A^\alpha} - \frac{1}{m_A^\gamma}}{\frac{m_B^\gamma}{m_A^\gamma} - \frac{m_B^\alpha}{m_A^\alpha}} \right\} \quad (3.63)
\end{aligned}$$

$$\Delta T = \frac{term1}{term2} \quad (3.64)$$

Note: In this calculation a symmetric phase diagram (all slopes equal,  $m_X^{\nu_i} = m$ ) is chosen and using the assumption of equal undercooling of all phases, that an expression for the global interface undercooling can be derived as  $\Delta T = 1/3(\Delta T_\alpha + \Delta T_\beta + \Delta T_\gamma)$  by elimination of the constants  $A_0$   $B_0$  using the relations  $(A_0 + B_0) = 0$ .

The average curvature undercooling is independent of the individual width of each lamellar, but depends only on the volume fraction and the number of lamellar of the specific phase. It is quite clear from the above examples that the final undercooling can always be written in standard form, where the last term of the  $\Delta T$  expression (which is proportional to  $1/\lambda$ ) can be computed for the case where all Gibbs-Thomson coefficients and liquidus slope. The detailed procedure to obtain the growth of three phase eutectic with

semi-brick structure has been described. The growth undercooling  $\Delta T$ , is expressed by the growth rate and structure size as

$$\Delta T = K_1 V \lambda + \frac{K_2}{\lambda} \quad (3.65)$$

# Chapter 4

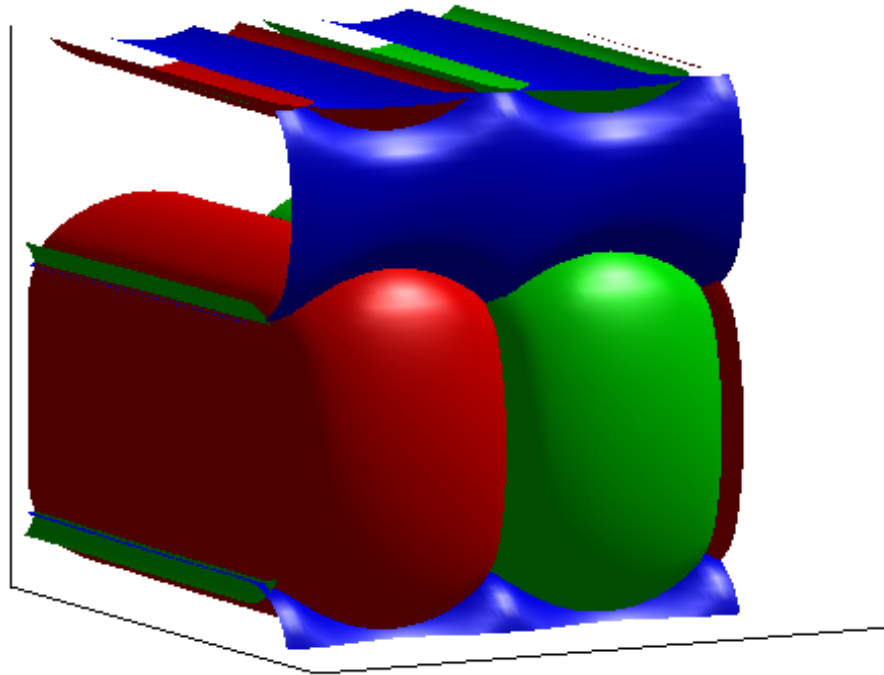
## Phase field simulation and parametric analysis

### 4.1 Algorithm for undercooling and lambda Calculations

From the Phase Diagram we can data for a ternary eutectic system

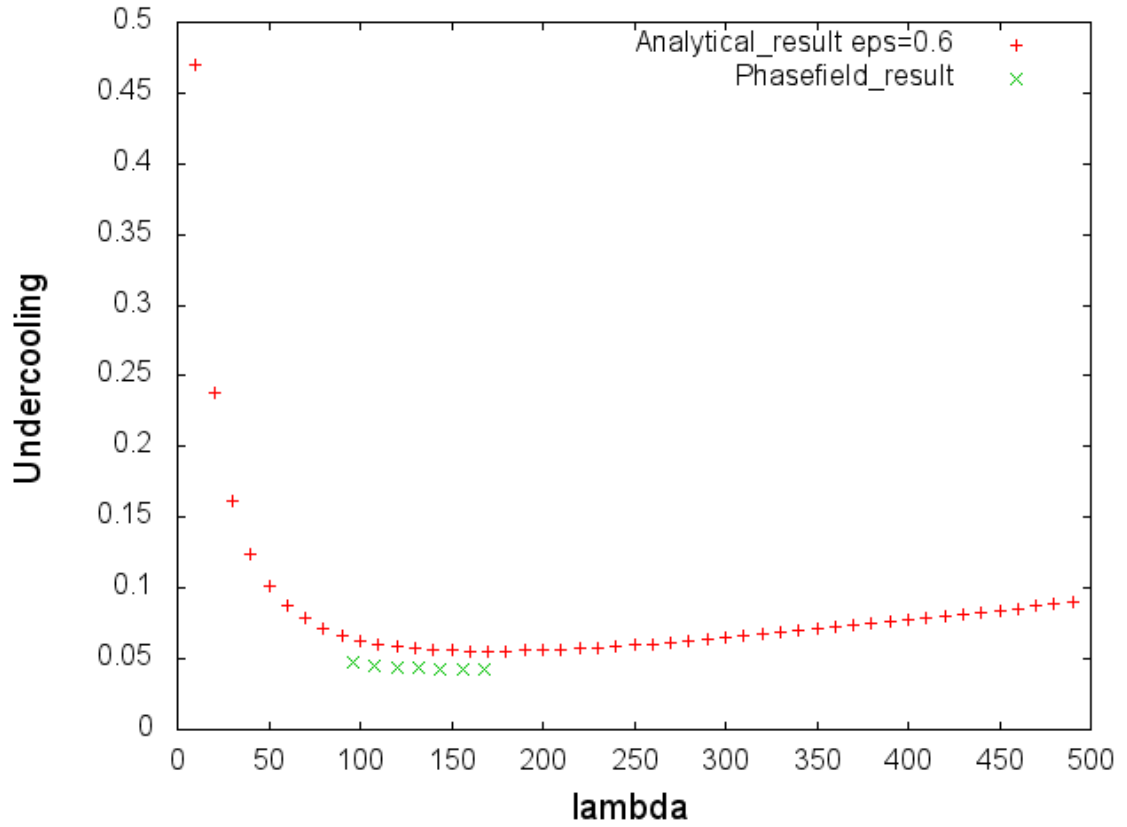
1. Calculate the volume fraction of  $\alpha, \beta$  and  $\gamma$  Phase.
2. Once the volume fraction is know the Domain of integration get fixed.
3. Calculate the Additional content difference.
4. Fix the Velocity ,Diffusion constant and epsilon.
5. Fix the contacts angles and Surface energy.
6. Calculate the Gibbs-Thomson contribution.
7. Slopes can be fixed fixed from the phase diagram.
8. Defining the additional functions for calculation of Fourier sum.
9. Calculate the average composition ahead of alpha beta and gamma phase.
10. Calculate term1 and term2 for each iterations 11. term1/term2 will give undercooling. 12. Undercooling vs Lambda can be plotted

## 4.2 Phase field simulation of evolution of semi-brick Structure



The figure show the result phase-field simulations and which is in agreement of the morphology seen in experiments.

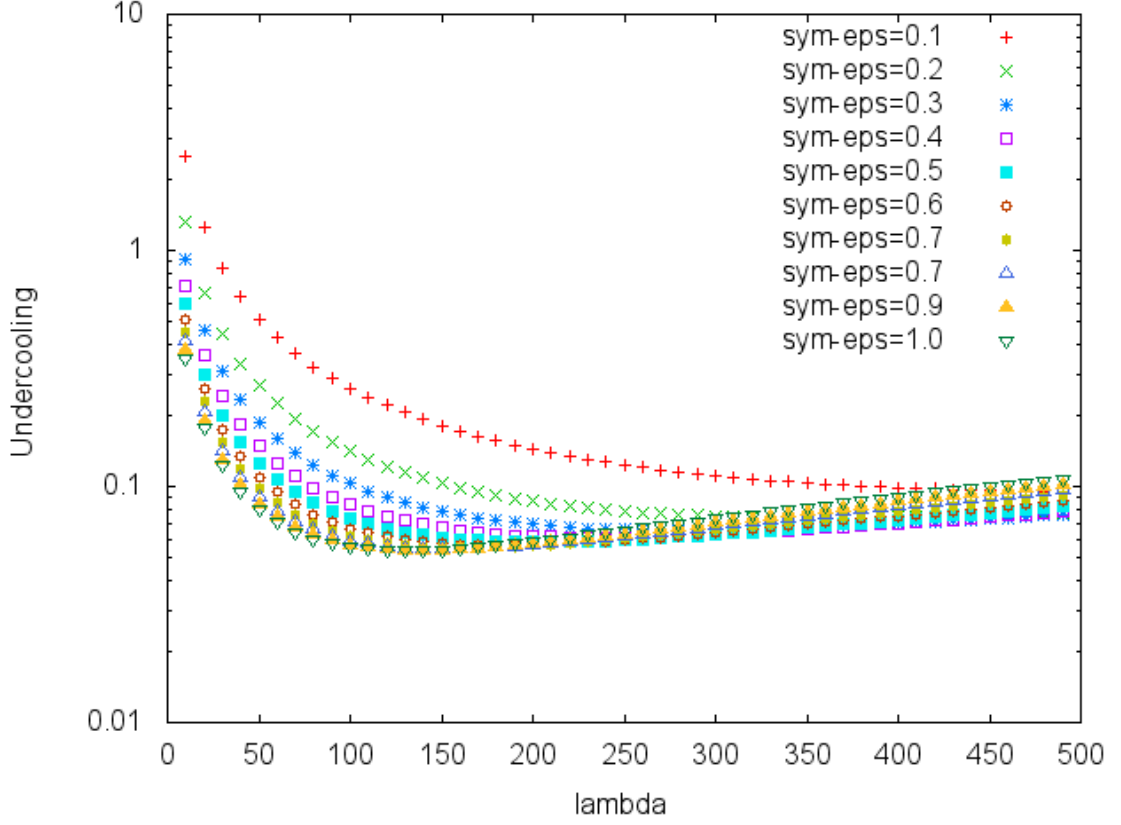
### 4.3 Comparison between: analytical and phase field results



From the above curve it is clear that the phase field simulation matches with the analytical results here seven data point are taken from the calculation based on the phase field model.

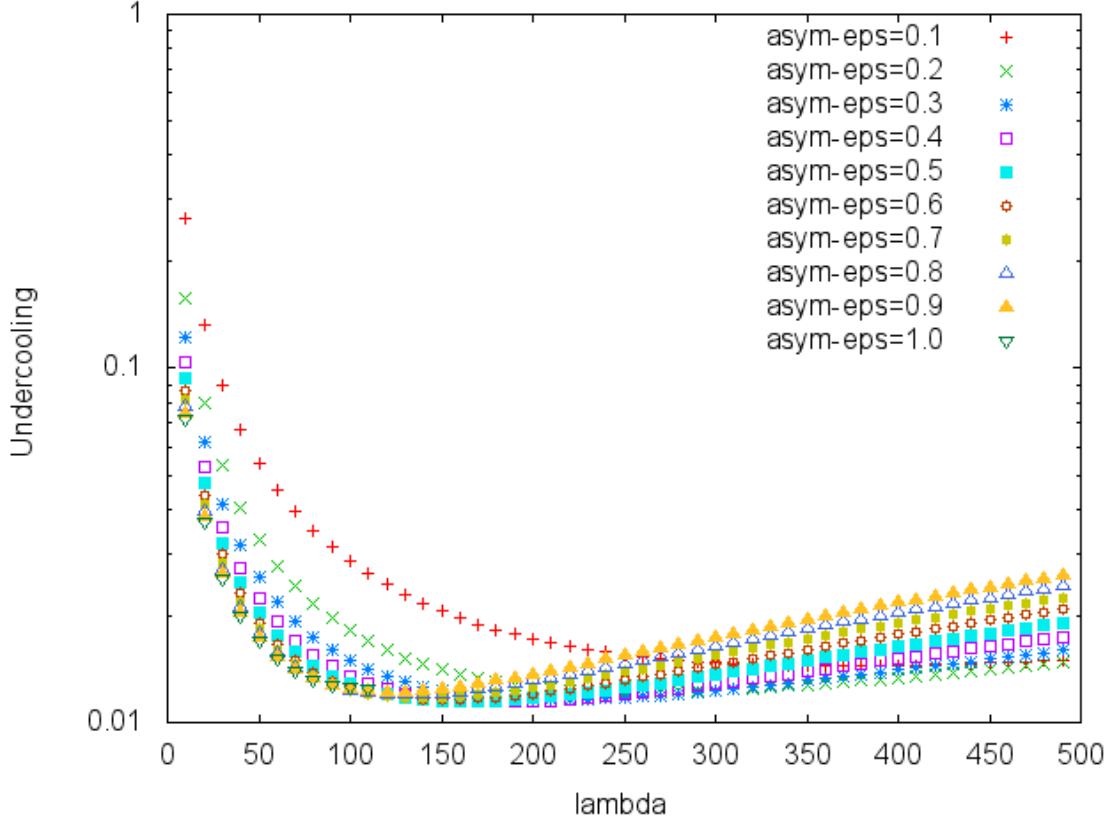


#### 4.4 Result for Symmetric phase diagram



From the above curves it is clear that as  $\epsilon = \lambda_{\alpha\beta+\gamma} / \lambda_{\alpha\beta}$  increases, the lambda minimum gets shifted towards the left i.e. to smaller values, and the corresponding  $\Delta T$  is getting closer to a smaller value.

## 4.5 Result For Non-Symmetric phase diagram

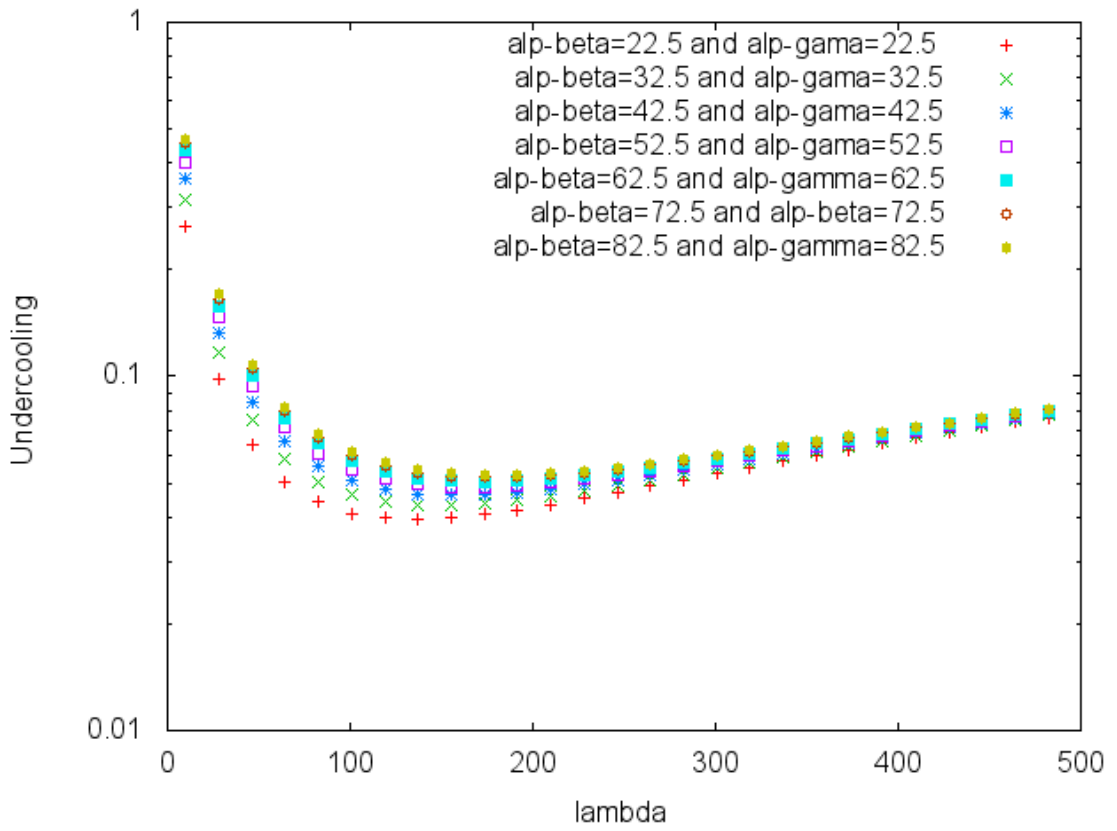


From the above curves it is clear that the as  $\epsilon = \lambda_{\alpha\beta+\gamma} / \lambda_{\alpha\beta}$  lambda minimum get shifted towards the left i.e to smaller and smaller value also the corresponding  $\Delta T$  is getting closer to smaller value that seem to be same as in case of symmertic but here the difference here is that undercooling is getting much more smaller value than the symmetric one. Also the lambda minimum in case of asymmertic one is centered around 100 whereas in symmetric case it is centered in between the 50 and 100

## 4.6 Parametric study : Undercooling vs $\lambda$ variation under the following parametric changes

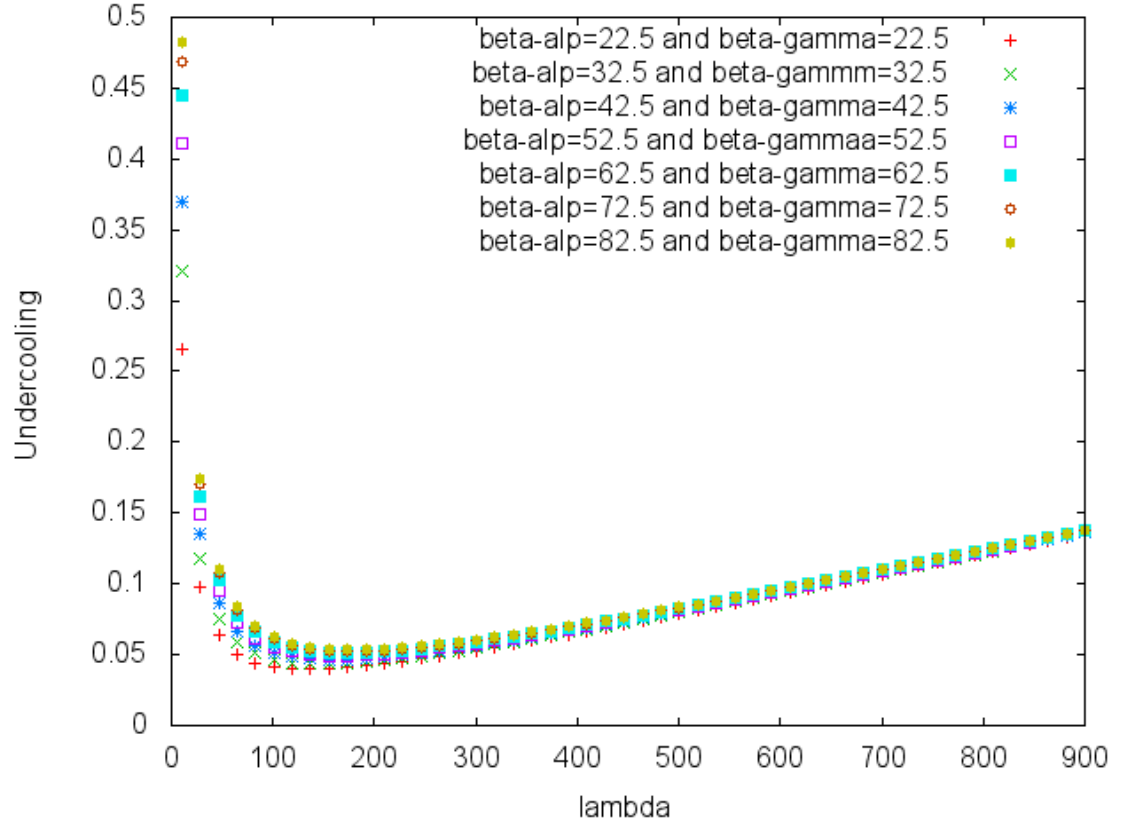
### 4.6.1 Influence of contact angle's(which get fixed by sufrace energy)

Variation in  $\theta_{\alpha\beta}$  and  $\theta_{\alpha\gamma}$



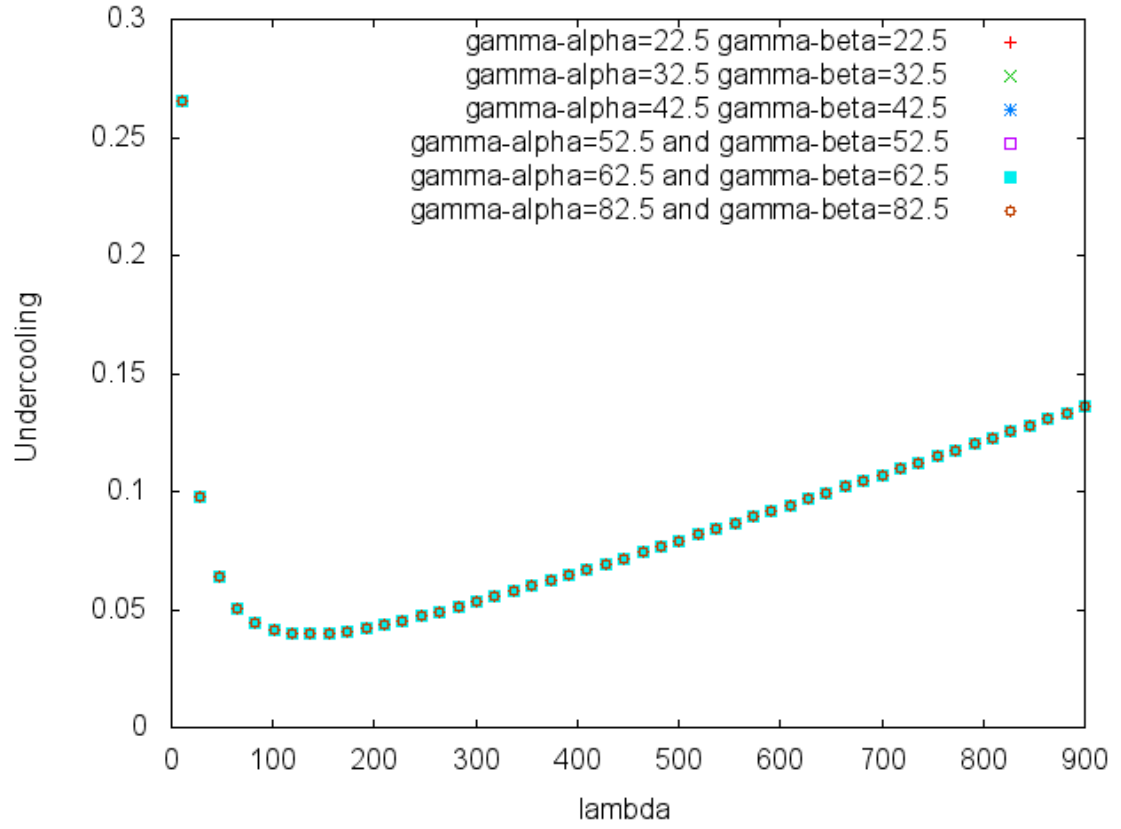
It is clear from the figure that changing contact angle has no effect on diffusion branch but there is significant change in capillarity branch. As the contact angle is increased the slope of capillarity branch decreases and there by increasing the undercooling value keeping the  $\lambda$  minimum fixed.

### Variation in $\theta_{\beta\alpha}$ and $\theta_{\beta\gamma}$



It is clear from the figure that changing contact angle has no effect on diffusion branch but there is significant change in capillarity branch. As the contact angle is increased the slope of capillarity branch decreases and there by increasing the undercooling value keeping the  $\lambda$  minimum fixed.

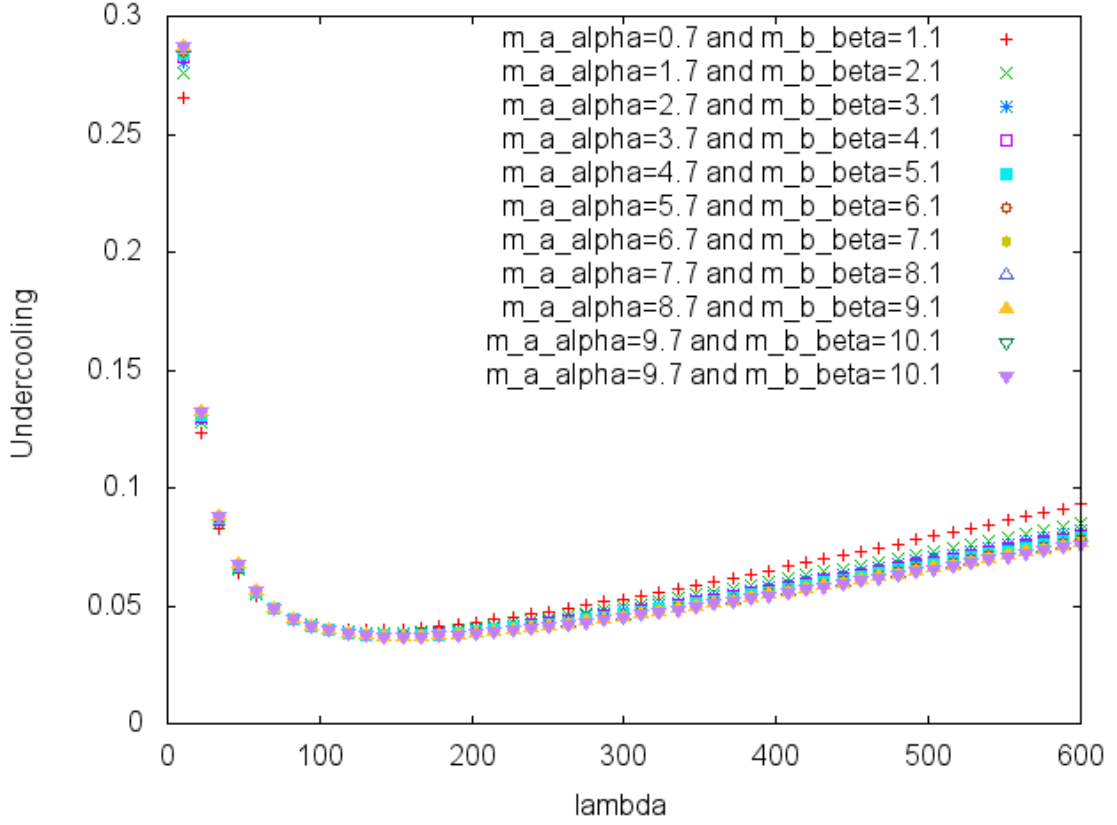
### Variation in $\theta_{\gamma\alpha}$ and $\theta_\gamma$



It is clear from the figure that changing contact angle has no effect on diffusion and capillarity branch. Plot for different contact angles are overlapping on each other.

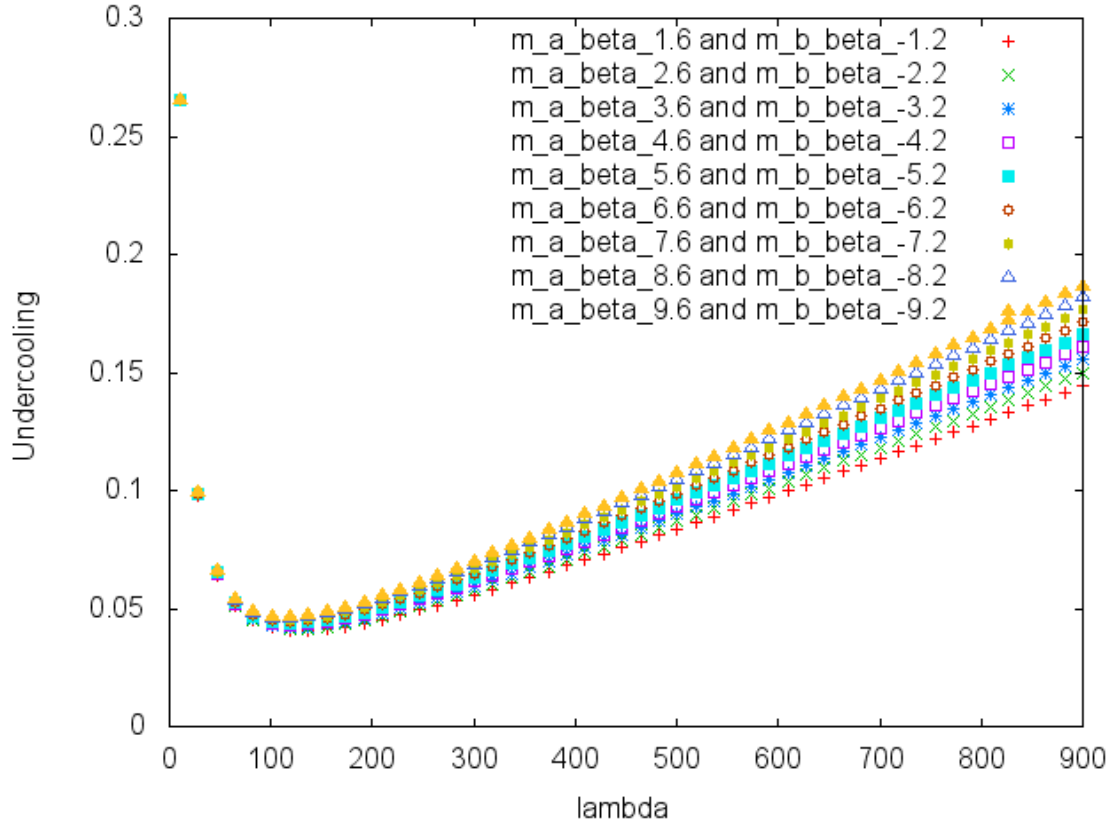
#### 4.6.2 Influence of slopes(liquidus)

$\alpha - l$  slope



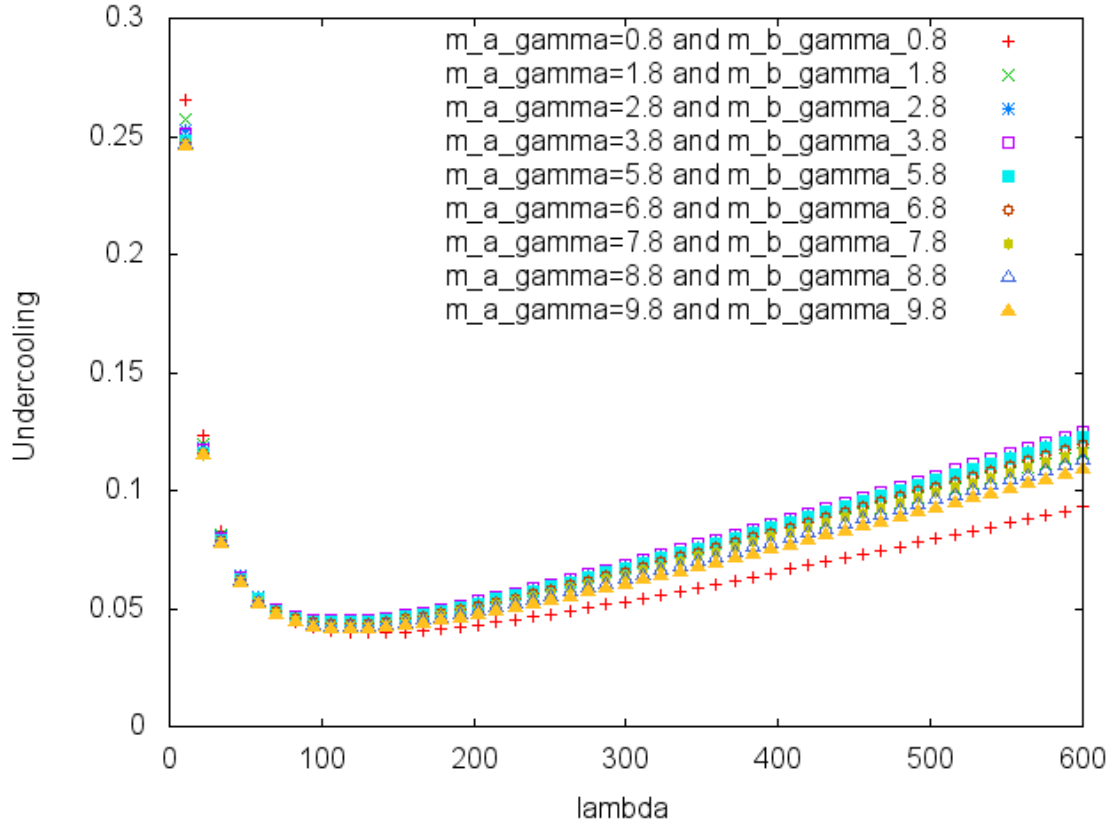
It is clear from the figure that changing contact angle has no effect on capillarity branch but there is significant change in diffusion branch. Now it is evident from the fig that as the value of slope increases, the slope of the Diffusion branch in the fig also decreases keeping the  $\lambda$  minimum fixed.

$\beta - l$  slope



It is clear from the figure that changing contact angle has no effect on capillarity branch but there is significant change in diffusion branch. Now it is evident from the fig that as the value of slope increases, the slope of the Diffusion branch in the fig increases keeping the lambda minimum fixed.

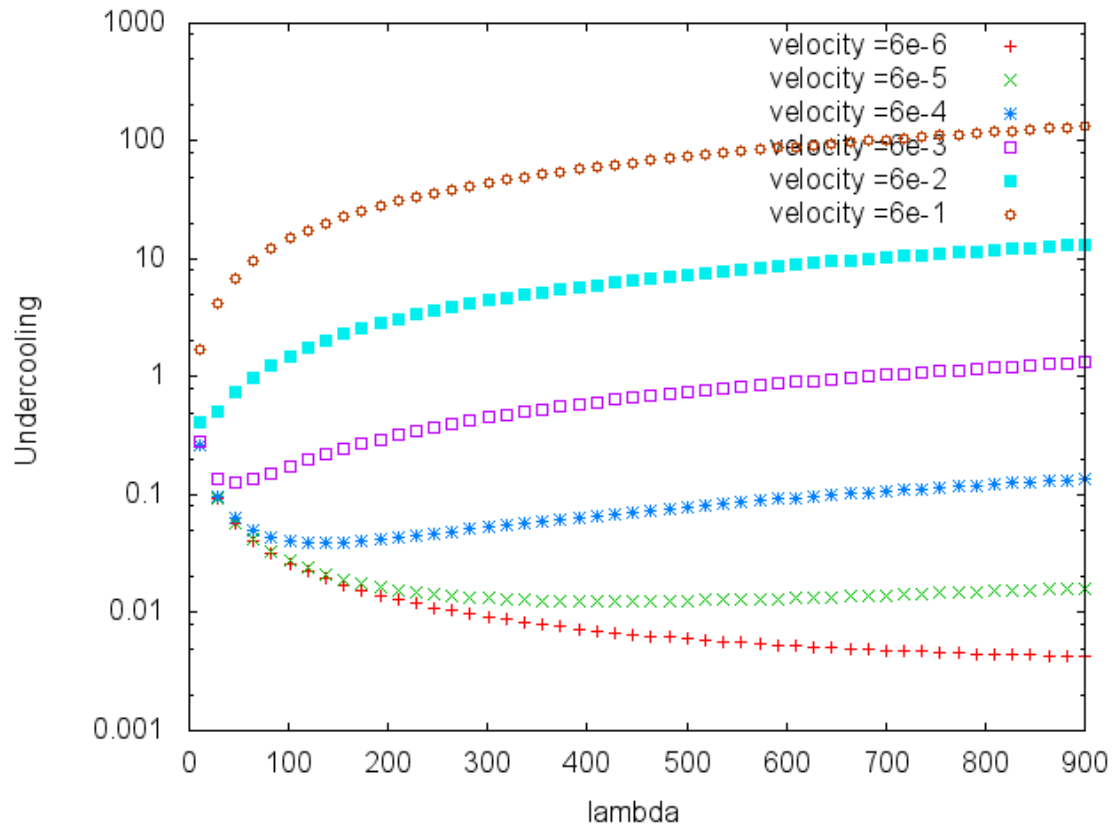
$\gamma - l$  slope



It is clear from the figure that changing contact angle has no effect of capillarity branch but there is significant change in diffusion branch. Now it is evident from the fig that as the value of slope increases, the slope of the Diffusion branch in fig first increases and then decreases as the lambda minimum is fixed.



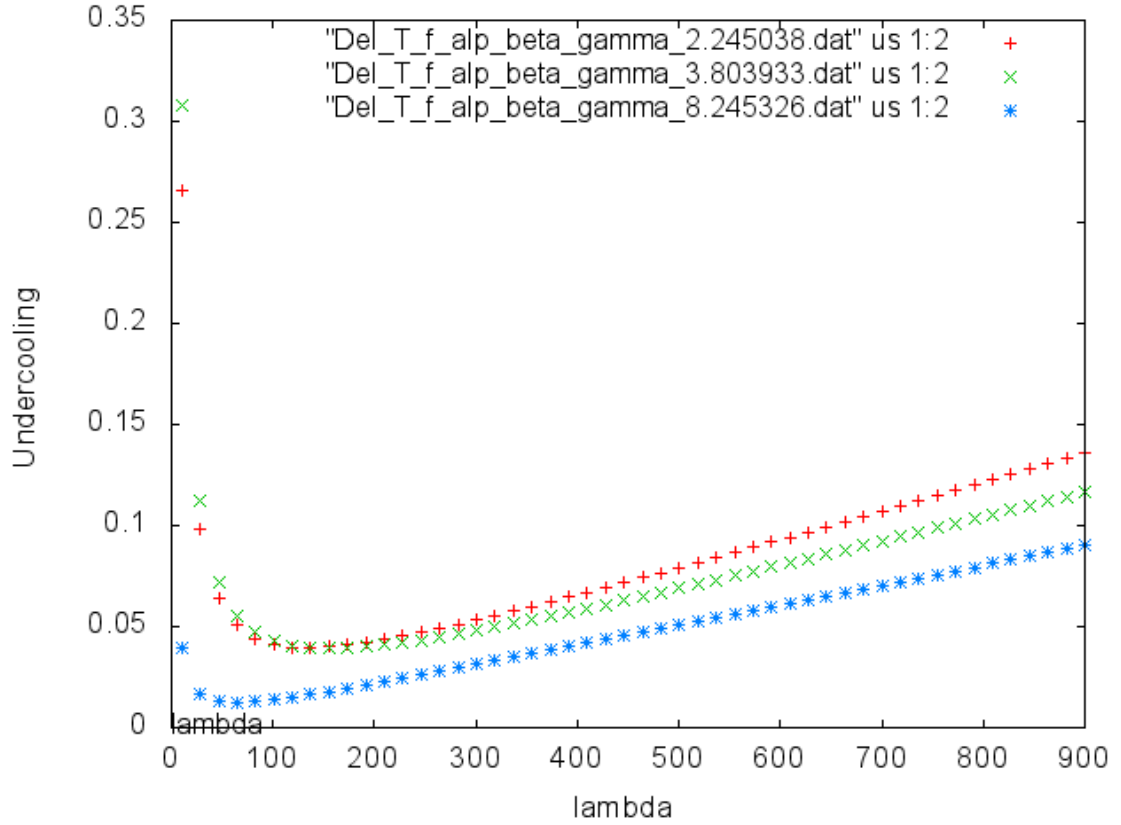
### 4.6.3 Influence of velocity



It can be observed that as velocity increases and especially for large velocity there is no longer a pattern for lambda min and  $\Delta T$  minimum

#### 4.6.4 Effect of Volume fractions

$\alpha$  and  $\beta$  phase growing in expense of  $\gamma$  phase



the ratio indicated in the figure is the ratio of volume fraction of  $\alpha +$  volume fraction of  $\beta$  is to volume fraction of  $\gamma$ . It is clear from the figure that as the volume fractions of  $\alpha$  and  $\beta$  phase increase, the volume fraction of  $\gamma$  starts decreasing and a point is reached where the binary eutectic is reached.

# Chapter 5

## Future Work

In order to estimate the undercooling and the spacing a suitable choice from the three models has been made. But for an easy estimate lamellar model is useful, regardless of the real morphology of the solidification structure. Here symmetry is used for calculations. In certain cases the symmetry is exact and general, which means the approximation will work fine but for non-symmetric phase diagrams, (real alloys) the symmetry can't be exactly realized because of asymmetries in the surface tensions, mobilities and liquidus slopes. Therefore some of the results of the parametric study can't be seen in experiments. In the present model convective mixing in liquid melt is not taken into consideration. So in future effect of solutal convection on spacing and undercooling selection in semi-regular structure can be done, where the parametric study of undercooling at the interface can be derived as a function of velocity with convection rate (that is lamellar flow vs turbulent flow) can be done.

## Chapter 6

### Conclusion

We can quantitatively compare the experiments micrograph and Phase field simulation result. It was found that the simulated micrograph is closest to the experimental micrograph after a suitable rotation of experimental micrograph. The influence of the volume fractions and surface energy on three-phase growth patterns has been studied and analysis showed that system selects a lambda minimum .

# Chapter 7

## Appendix

The detailed procedure to obtain the growth of three phase eutectic with semi-brick structure has been described. The growth undercooling  $\Delta T$ , is expressed by the growth rate and structure size as

$$\Delta T = K_1 V \lambda + \frac{K_2}{\lambda} \quad (7.1)$$

### 7.1 Appendix A

Appendix: The symbol of the slopes of the liquidus surface  $L+\alpha, L+\beta$  and  $L+\gamma$ , let's introduce the most natural definition for the slopes of the liquidus surface. First we will define the symbol for the slope of the  $L+\alpha$  surface. If the equilibrium temperature of a point on the surface at the eutectic point drops  $m_B^\alpha K$  when it moves 1% along the unit vector  $\vec{b}$ , then slope of the liquidus  $L+\alpha$  along the  $\vec{b}$  is defined as  $m_B^\alpha$  K%. That is we define  $m_B^\alpha$  as

$$m_B^\alpha = \left( \frac{\partial T_\alpha^L}{\partial C_B} \right) |_{C_C} \quad (7.2)$$

similarly, we can define  $m_C^\alpha$  as

$$m_C^\alpha = \left( \frac{\partial T_\alpha^L}{\partial C_C} \right) |_{C_B} \quad (7.3)$$

using the vector  $\vec{c}$

We shall define the slopes of the liquidus surface  $L+\beta$  along  $\vec{a}$  and  $\vec{c}$  as  $m_A^\beta$  and  $m_C^\beta$  that is

$$m_A^\beta = \left( \frac{\partial T_\beta^L}{\partial C_A} \right) |_{C_C} \quad (7.4)$$

and

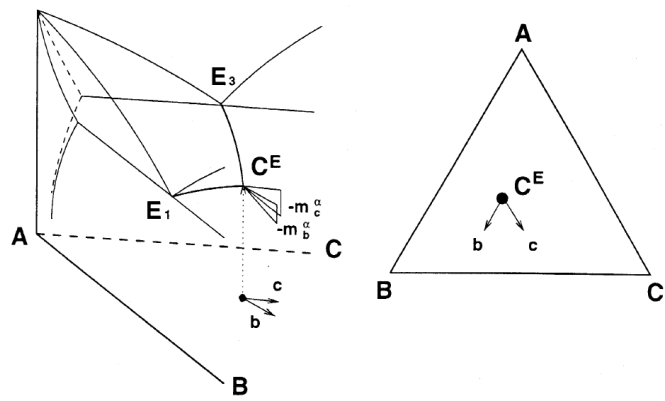
$$m_C^\beta = \left( \frac{\partial T_\beta^L}{\partial C_C} \right) |_{C_A} \quad (7.5)$$

Similarly, we shall define the slopes of the liquidus surface L+ $\gamma$  along  $\vec{a}$  and  $\vec{b}$  as  $m_A^\gamma$  and  $m_B^\gamma$ . That is

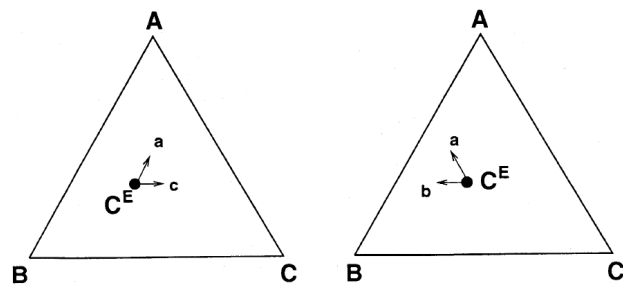
$$m_A^\gamma = \left( \frac{\partial T_\gamma^L}{\partial C_A} \right) |_{C_B} \quad (7.6)$$

and

$$m_B^\gamma = \left( \frac{\partial T_\gamma^L}{\partial C_B} \right) |_{C_A} \quad (7.7)$$



(a)



(b)

## 7.2 Appendix B

The relation of initial alloy composition and the volume fraction of each phase.

The initial composition  $(C_B^L, C_C^L)$ . It solidifies to form  $\alpha$  phase  $(C_{OB}^\alpha, C_{OC}^\alpha)$ ,  $\beta$  phase  $(C_{OB}^\beta, C_{OC}^\beta)$ ,  $\gamma$  phase  $(C_{OB}^\gamma, C_{OC}^\gamma)$ . The volume fraction of the three phase are denoted by  $f_\alpha, f_\beta$  and  $f_\gamma$  respectively. Three equation are given as

$$C_B^L = f_\alpha C_{OB}^\alpha + f_\beta C_{OB}^\beta + f_\gamma C_{OB}^\gamma \quad (7.8)$$

$$C_C^L = f_\alpha C_{OC}^\alpha + f_\beta C_{OC}^\beta + f_\gamma C_{OC}^\gamma \quad (7.9)$$

$$C_A^L = f_\alpha C_{OA}^\alpha + f_\beta C_{OA}^\beta + f_\gamma C_{OA}^\gamma \quad (7.10)$$

$$f_\alpha + f_\beta + f_\gamma = 1 \quad (7.11)$$

If  $(C_{OB}^\alpha, C_{OC}^\alpha), (C_{OB}^\beta, C_{OC}^\beta)$  and  $(C_{OB}^\gamma, C_{OC}^\gamma)$  are assumed approximately to be those of their solubility limits, then  $f_\alpha, f_\beta$  and  $f_\gamma$  can be determined when  $(C_B^L, C_C^L)$  is given. Molar volume of the three phases have to be equal when the compositions are expressed with at %, or the densities of the three phase have equal when the composition are expressed with mass%. These assumptions are not exactly true to real ternary eutectic system, but adequate as a first approximation.



# References

- [1] K.A. Jackson and J.D. Hunt Tans. Metall. Soc. AIME 226, 1129 (1966)
- [2] T.Himemiya and T. Umeda, Mater. Trans.,JIM 40,665(1999)
- [3] Abhik Choudhury,Mathis Plapp and Britta Nestler, Physical Review E 83, 051608 (2011)
- [4] Abhik Choudhury,Y.C. Yabansu,S.R. Kalidindi,A. Dennstedt, Acta Materialia 110 (2016) 131-141